INS-NUMA-49

Equipments for Momentum Cooling at TARN

H.Yonehara, N.Tokuda,
M.Yoshizawa and T.Hattori

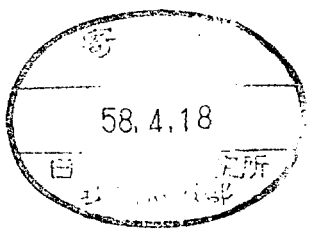

March, 1983

STUDY GROUP OF NUMATRON AND
HIGH-ENERGY HEAVY-ION PHYSICS
INSTITUTE FOR NUCLEAR STUDY
UNIVERSITY OF TOKYO
Midori-Cho 3-2-1, Tanashi-Shi,
Tokyo 188, Japan

INS-NUMA-49

March 1983

Equipments for Momentum Cooling at TARN

H. Yonehara, N. Tokuda, M. Yoshizawa and T. Hattori

Institute for Nuclear Study, University of Tokyo

3-2-1 Midori-cho, Tanashi-shi, Tokyo, Japan

Contents ;

1. Introduction

The present paper is dedicated to designing and preparing the experimental equipments for the momentum cooling at TARN [1].

Stochastic cooling has been the subject of much theoretical and experimental work [2,3,4,5,6], and recently this method is applied to accumulate anti-proton and make high luminosity beam of anti-proton at CERN and Fermi National Laboratory [7,8,9].

Application of this method to the beam stacked in TARN which is a storage ring for accumulation test of heavy ion attached to SF cyclotron at Institute for Nuclear Study, Univ. of Tokyo, and the equipments for longitudinal momentum cooling with filter method have been set up. The specification of TARN is shown in Table 1-1, and the number of stacked protons is measured to be about 10^8 particles maximum. The life time of the 7 MeV proton beam in the ring is about 400 sec at 1×10^{-10} Torr.

2. Review of Momentum Cooling Theory and Study of Betatron Oscillation Blow-up

2-1. Momentum Cooling Rate

After one kick, the root-mean-square of momentum distribution of the whole particles Z changes as described by a differential equation [2,3] by

$$\frac{dZ}{dt} = \frac{W}{2N}\left[(-2g+g^2)Z + g^2R^2\frac{1}{Z}\right] \qquad (2\text{-}1\text{-}1)$$

where,

N ; number of the whole particles

W ; bandwidth of the feedback system

$$Z = Z_{rms} = \left[\frac{1}{N} \sum_{ij}^{N} z_{ij}^2 \right]^{1/2}$$

$$z_{ij} = p_{ij} - p_0 \qquad (2\text{-}1\text{-}2)$$

p_0 ; nominal momentum .

To derive Eq. (2-1-1) we assume the j-th particle in the i-th sample is kicked at the kicker as

$$z_{ij} - g(\bar{z}_i + \bar{r}_i) ,$$

g ; gain of the system

$\bar{r}_i$; thermal noise

$$R = r_{rms} = \left[\frac{1}{N} \sum_{i}^{N_s} \bar{r}_i^2 \right]^{1/2}$$

$$N_s = W/f_0$$

f_0 ; revolution frequency .

Now writing the ratio of the thermal noise power to signal power at the initial state $Z_0 = Z(0)$ as h_0 ,

$$h_0 = \frac{R^2}{Z_0^2} , \qquad (2\text{-}1\text{-}3)$$

we have

$$\frac{dZ}{dt} = \frac{W}{2N} \left[(-2g + g^2) Z + g^2 h_0 \frac{Z_0^2}{Z} \right] . \qquad (2\text{-}1\text{-}4)$$

The initial e-folding time is

$$\tau_i = \frac{2N}{W} / \left[2g - g^2 (1 + h_0) \right] , \qquad (2\text{-}1\text{-}5)$$

and is optimized to

$$\tau_0 = \frac{2N}{W}\left(1 + h_0\right) \qquad (2\text{-}1\text{-}6)$$

with

$$g = \frac{1}{1 + h_0} \equiv g_0 \quad . \qquad (2\text{-}1\text{-}7)$$

Assuming $h_0 >> 1$ as in a usual case and defining G by

$$G \equiv \frac{g}{g_0} \quad , \qquad (2\text{-}1\text{-}8)$$

we have a solution

$$Z(t) = Z_0 \left[\left(1 - \frac{G}{2}\right) e^{-4Gt/\tau_0} + \frac{G}{2}\right]^{\frac{1}{2}} \qquad (2\text{-}1\text{-}9)$$

$$Z(\infty) = Z_0 \left[G/2\right]^{\frac{1}{2}} \quad . \qquad (2\text{-}1\text{-}10)$$

The solutions for some values of G are drawn in Fig. 2-1 . It should be noted that G must be reduced to attain small final momentum spread in cost of cooling time.

In the above calculation, G is kept constant throughout the cooling process. Here we introduce time varying g

$$g(t) = \frac{1}{1 + h_0 Z_0^2/Z^2} \qquad (2\text{-}1\text{-}11)$$

to attain minimum e-folding time at any time. Then Eq. (2-1-4) reduces to

$$\frac{dZ}{dt} = -\frac{W}{2N}\frac{1}{1 + h_0(Z_0^2/Z^2)} \quad . \qquad (2\text{-}1\text{-}12)$$

With $h_0 >> 1$, we have

$$Z(t) = Z_0 \left[\frac{2t}{\tau_0} + 1\right]^{\frac{1}{2}} \quad , \qquad (2\text{-}1\text{-}13)$$

which is drawn in Fig. 2-1. We can attain a short cooling time and small final momentum spread with this time varying gain, but

it is technically difficult to realize it.

2-2. Power Estimation

Energy spread of the beam is described with its momentum p,

$$\frac{\Delta E}{E} = 2\,\frac{\Delta p}{p} \qquad (2\text{-}2\text{-}1)$$

and

$$\frac{\Delta f}{f} = \left(\frac{1}{\gamma^2} - \frac{1}{\gamma_{tr}^2}\right)\frac{\Delta p}{p} \quad . \qquad (2\text{-}2\text{-}2)$$

Now, $\gamma \sim 1$, $\gamma_{tr} \sim 2$, and the frequency spread Δf is assumed about 30 kHz i.e.,

$$[\ \Delta p/p\ ] \sim 3.6\ \%$$

then, the energy spread ΔE is

$$\Delta E \sim 0.51\ \text{MeV} \quad .$$

Assuming the whole number $N \sim 10^9$ particles and the length of the sample ~ 60 cm, particle number in one sample is 2×10^7 particles. Then the root-mean-square of the energy error of a sample (2×10^7 particles) is

$$\frac{0.51 \times 10^6}{\sqrt{2 \times 10^7}} = 0.114 \times 10^3\ \text{eV} \quad .$$

Then the required signal voltage ΔE_c [3] is

$$\Delta E_c = g_0 \times 0.114 \times 10^3$$
$$= 46.5\ \text{V for } g_0 = 0.408 \text{ i.e., } h_0 = 1.45 \quad .$$

If the impedance of the kicker is 100 Ω , the power which makes particles correction is

$$P = \frac{46.5^2}{100} = 21.6 \text{ Watt.} \quad , \tag{2-2-3}$$

and the noise power,

$$h_0 P = 1.45 \times 21.6 = 31.4 \text{ Watt.} \quad . \tag{2-2-4}$$

Then the total power of the main amplifier needs 53 Watt. however, considering the betatron oscillation blow-up described below, the power at the kicker must be reduced.

2-3. Blow-up

Vertical phase space

When a particle is accelerated or decelerated at the kicker, its y'=dy/dz changes as

$$y' \to y'\left(1 - \frac{p}{p_0}\right) \tag{2-3-1}$$

$$\Delta p = -g\left(\bar{z}_i + \bar{r}_i\right) \quad . \tag{2-3-2}$$

We assume the motion of a particle in the vertical phase space is described by

$$\gamma y_{ij}^2 + \frac{1}{\gamma} y'^2_{ij} = \frac{\varepsilon_{ij}}{\pi} \equiv E_{ij} \quad , \tag{2-3-3}$$

where γ is the ellipse parameter. Then the root-mean-square of the emittance changes after one kick to the whole particles as follows

$$\Delta(E^2) = \frac{1}{N} \sum_{ij}^{N} \left[\gamma y_{ij}^2 + \frac{1}{\gamma} (1-\rho_i)^2 y'^2_{ij} \right] - \frac{1}{N} \sum_{ij}^{N} E_{ij}^2 \quad , \tag{2-3-4}$$

where

$$\rho_i = \frac{\Delta p}{p_0} \quad . \tag{2-3-5}$$

Transforming y'_{ij} to

$$\Delta(E^2) = \frac{2}{N} \sum \rho_i^2 \left(E_{ij}^2 \cos^2\phi_{ij} + 2E_{ij}^2 \cos^4\phi_{ij} \right)$$

$$\sim \frac{5}{2} \frac{1}{N} \sum_{ij}^{N} \rho_i^2 \cdot E_{ij}^2 \quad . \tag{2-3-6}$$

As there is no correlation between ρ_i and E_{ij}, this equation is

$$\Delta(E^2) = \frac{5W}{2Nf_0} \frac{g^2}{p_0^2} \left(Z^2 + R^2 \right) E^2 \quad . \tag{2-3-7}$$

The resultant differential equation is

$$\frac{dE}{dt} = \frac{5}{4} \frac{W}{N} \frac{g^2}{p_0^2} \left(Z^2(t) + R^2 \right) E \quad . \tag{2-3-8}$$

Under usual condition $h_0 >> 1$, this equation is written as

$$\frac{dE}{dt} = \frac{5}{2} \left(\frac{Z_0}{p_0} \right)^2 \frac{G^2}{h_0} \frac{1}{\tau_0} \left[\left(1 - \frac{G}{2} \right) e^{-4Gt/\tau_0} + h_0 \right] E \quad , \tag{2-3-9}$$

the solution is

$$E(t) = E_0 \exp\left[\frac{5}{2} \left(\frac{Z_0}{p_0} \right)^2 \frac{G^2}{h_0} \left\{ \frac{1}{4G} \left(1 - \frac{G}{2} \right) \left(1 - e^{-4Gt/\tau_0} \right) + h_0 \frac{t}{\tau_0} \right\} \right] \tag{2-3-10}$$

in shown as Fig. 2-2 for the case of h_0=10 and G=1. This figure shows that the blow-up of vertical betatron oscillation is not a severe problem even with G=1.

Horizontal phase space

The position of a particle in a horizontal phase space changes at the kicker by

$$x_{ij} \rightarrow x_{ij} + \eta\frac{\Delta p}{p_0}$$

$$x'_{ij} \rightarrow x'_{ij}\left(1 - \frac{\Delta p}{p_0}\right) ,$$

where η is a dispersion function. With a calculation similar to the above one, we have

$$\Delta(E^2) = \frac{W}{Nf_0}\frac{g^2(Z^2+R^2)}{p_0^2}\left[\,4\gamma\eta^2 E + \frac{5}{2}E^2\,\right] . \qquad (2\text{-}3\text{-}11)$$

As the first term in the bracket is leading, the following equation derived

$$\frac{dE}{dt} = 4\left(\frac{Z_0}{p_0}\right)^2 \gamma\eta^2\frac{G^2}{h_0}\,\frac{1}{\tau_0}\left[\left(1-\frac{G}{2}\right)e^{-4Gt/\tau_0} + h_0\right] , \qquad (2\text{-}3\text{-}12)$$

where constant G and $h_0 \gg 1$ are assumed. This provides

$$E(t)=E_0\left(1+4\left(\frac{Z_0}{p_0}\right)^2\frac{\gamma\eta^2 G^2}{E_0 h_0}\left[\frac{1}{4G}\left(1-\frac{G}{2}\right)\left(1-e^{-4Gt/\tau_0}\right)+h_0\frac{t}{\tau_0}\right]\right), \qquad (2\text{-}3\text{-}13)$$

As Fig. 2-3 shows horizontal emittance blow up is a severe problem, so far as G is not reduced.

With time varying G defined by Eq. (2-1-4), the equation of blow-up is

$$\frac{dE}{dt} = \frac{4}{\tau_0}\left(\frac{Z_0}{p_0}\right)^2\gamma\eta^2\,\frac{1}{(2t/\tau_0+1)^2} , \qquad (2\text{-}3\text{-}14)$$

where $h_0 \gg 1$ is assumed. The solution is

$$E = E_0\left[\,2\left(\frac{Z_0}{p_0}\right)^2\frac{\gamma\eta^2}{E_0}\left(1-\frac{1}{(2t/\tau_0+1)}\right)+1\,\right] . \qquad (2\text{-}3\text{-}15)$$

Fig. 2-3 shows a solution in the case of $Z_0/p_0 = 0.0075$, $\gamma = 1.14\ m^{-1}$, $\eta = 1.2$ m and $E_0 = 80$ mm·mrad, where

$$E(\infty)/E_0 = 3.3 . \qquad (2\text{-}3\text{-}16)$$

3. Beam Pickup and Kicker

Travelling wave coupler [10] with the structure of helix was chosen as the beam signal pickup monitor and the kicker, because the phase velocity of the picked up signal along the travelling wave helix coupler is agreed with the beam velocity, and the coupler has advantage of good signal to noise ratio. The coupling impedance and the total gain of the T.W. helix coupler is calculated with the sheath helix model [11,12,13,14].

3-1. Coupling Impedance and Total Gain

Coupling Impedance, the total gain and the electric field distribution of the T.W. helix monitor are calculated in the axial coordinate with Maxwell equations, equation of motion and the sheath helix model [12,13,14] assuming that the beam current column and the helix are co-axial. With the parameters shown in Fig. 3-1, the radial component of the electric field at the axial point z, $E_z(r)$, is

i) inside the beam column $(0 \leqq r < a)$

$$\frac{1}{r}\frac{\partial}{\partial r}\left(r \frac{\partial E_z}{\partial r} \right) + \gamma_s^2 E_z = 0 \quad (\gamma_s^2 > 0) \qquad (3\text{-}1\text{-}1)$$

ii) outside the beam column $(a \leqq r \leqq b)$

$$\frac{1}{r}\frac{\partial}{\partial r}\left(r \frac{\partial E_z}{\partial r} \right) - \gamma_0^2 E_z = 0 \quad (\gamma_0^2 > 0) \qquad (3\text{-}1\text{-}2)$$

where.

γ_s , γ_0 ; propagation constants,

$$\gamma_0^2 = \beta_0^2 - k^2 = \omega^2\left(\frac{1}{v^2} - \frac{1}{c^2}\right) = \frac{\omega^2}{c^2}\left(\frac{1}{\beta_v^2} - 1\right) ,$$

$v = c\beta_v$; beam velocity,

a ; radius of the beam column,

b ; radius of the outer-conductor .

The solutions of Eqs. (3-1-1) and (3-1-2) are represented respectively with the 0-th Bessel function $J_0(\gamma_s r)$, and the 0-th modified Bessel functions $I_0(\gamma_0 r)$ and $K_0(\gamma_0 r)$. Then,

$$\text{i)}\quad E_z = E_{z1} = AJ_0(\gamma_s r) \qquad (0 \leqq r < a) \qquad (3\text{-}1\text{-}3)$$

$$\text{ii)}\quad E_z = E_{z2} = CI_0(\gamma_0 r) + DK_0(\gamma_0 r) \qquad (a \leqq r \leqq b) \qquad (3\text{-}1\text{-}4)$$

The two solutions must be continuous at the point r=a, then,

$$-\frac{\gamma_s a J_1(\gamma_s a)}{J_0(\gamma_s a)} = \gamma_0 a \frac{I_1(\gamma_0 a)K_0(\gamma_0 b) + I_0(\gamma_0 b)K_1(\gamma_0 a)}{I_0(\gamma_0 a)K_0(\gamma_0 b) - I_0(\gamma_0 b)K_0(\gamma_0 a)} . \qquad (3\text{-}1\text{-}5)$$

Defining and drawing two functions;

$$y = \frac{J_1(x)}{J_0(x)} \qquad (3\text{-}1\text{-}6)$$

and

$$y = -\frac{1}{x}\gamma_0 a \frac{I_1(\gamma_0 a)K_0(\gamma_0 b) + I_0(\gamma_0 b)K_1(\gamma_0 a)}{I_0(\gamma_0 a)K_0(\gamma_0 B) - I_0(\gamma_0 b)K_0(\gamma_0 a)} \qquad (3\text{-}1\text{-}7)$$

the values of $x = \gamma_s a$ are given as the cross points of the two figures, and γ_s's are obtained. Because γ_s's mean the periods of the vibration of the radial electric field $E_z(r)$ in the beam, the lowest γ_s's are used as follows. Reducing the coefficients A, C and D, we have

$$\text{i)}\quad E_{z1}(r) = E_{z1}(0)J_0(\gamma_s r) \qquad (0 \leqq r \leqq a) \qquad (3\text{-}1\text{-}8)$$

ii) $$E_{z2}(r) = \frac{E_{z1}(0)J_0(\gamma_s a)\,[K_0(\gamma_0 b)I_0(\gamma_0 r) - I_0(\gamma_0 b)K_0(\gamma_0 r)]}{K_0(\gamma_0 b)I_0(\gamma_0 a) - I_0(\gamma_0 b)K_0(\gamma_0 a)} \quad (3\text{-}1\text{-}9)$$

$$(a \leqq r \leqq b)$$

At the helix ($r=\ell$; $a \leqq \ell \leqq b$)

$$E_{z2}(\ell) = \frac{E_{z1}(0)J_0(\gamma_s a)\,[K_0(\gamma_0 b)I_0(\gamma_0 \ell) - I_0(\gamma_0 b)K_0(\gamma_0 \ell)]}{K_0(\gamma_0 b)I_0(\gamma_0 a) - I_0(\gamma_0 b)K_0(\gamma_0 a)} \quad (3\text{-}1\text{-}10)$$

where ℓ is the helix radius. With Eq. (3-1-8), the beam current I_1 is represented [11] ,

$$I_1 = \int_0^a 2\pi r i_1 \, dr = \int_0^a 2\pi r \frac{j\omega\varepsilon_0\omega_p^2}{(\omega-\beta v_0)^2} E_{z1} \, dr$$

$$= \frac{j\omega\varepsilon_0\omega_p^2}{(\omega-\beta v_0)^2} E_{z1}(0) \int_0^a 2\pi r J_0(\gamma_s r) \, dr \quad . \quad (3\text{-}1\text{-}11)$$

Then, the coupling impedance $|Z_c|$ is given by

(3-1-12)

$$|Z_c| = \left|\frac{E_{z2}(\ell)}{I_1}\right|$$

$$= J_0(\gamma_s a) \frac{K_0(\gamma_0 b)I_0(\gamma_0 \ell) - I_0(\gamma_0 b)K_0(\gamma_0 \ell)}{K_0(\gamma_0 b)I_0(\gamma_0 a) - I_0(\gamma_0 b)K_0(\gamma_0 a)} \frac{\gamma_0^2}{\omega\varepsilon_0(\gamma_s^2+\gamma_0^2)} \frac{\gamma_s}{2\pi a J_1(\gamma_s a)}$$

where, the relation [11] of

$$\frac{(\omega - \beta v_0)^2}{\omega_p^2} = \frac{\gamma_0^2}{\gamma_s^2 + \gamma_0^2} \quad (3\text{-}1\text{-}13)$$

is used.

Next, using the propagation constant of the helix Γ_c [10]

$$dV(z_d) = dV(z) \, e^{-\Gamma_c (z_d - z)} \quad , \quad (3\text{-}1\text{-}14)$$

z_d ; coupler length .

With $E_{z2}(\ell)$ induced per unit length by the beam current, we have

$$dV(z) = E_{z2}(\ell)\, e^{-\Gamma\cdot z}\, dz \quad , \tag{3-1-15}$$

$$\Gamma = \frac{j\omega}{\beta_c c} \quad ; \quad \text{propagation constant of the beam} \quad .$$

Then, at the end point,

$$V(\ell) = \int_0^{z_d} dV(z_d) = \int_0^{z_d} dV(z)\, e^{-\Gamma_c(z_d - z)}$$

$$= \int_0^{z_d} E_{z2}(\ell)\, e^{-\Gamma_c z_d - (\Gamma - \Gamma_c)\cdot z}\, dz$$

$$= E_{z2}(\ell)\, e^{-\Gamma_c z_d} \frac{1}{\Gamma_c - \Gamma} \left[e^{(\Gamma_c - \Gamma)\cdot z_d} - 1 \right] \quad . \tag{3-1-16}$$

The transfer function G is given by

$$G = \frac{V(\ell)}{I_1\, e^{-\Gamma\cdot z_d}} = Z_c \frac{1}{\Gamma_c - \Gamma} \left[1 - e^{-(\Gamma_c - \Gamma) z_d} \right] \tag{3-1-17}$$

where,

$$\Gamma_c = j\frac{d\phi}{dz} = j\frac{2}{z_c}\sin^{-1}\frac{\omega}{\omega_c} \tag{3-1-18}$$

$$\omega_c = \frac{v\pi}{\ell_c}$$

$$\Gamma = j\frac{\omega}{\beta_c c} \quad . \tag{3-1-19}$$

Using A which is defined by

$$jA = (\Gamma_c - \Gamma)\cdot z_d = j\left[2\frac{z_d}{z_c}\sin^{-1}\frac{\omega}{\omega_c} - \frac{\omega z_d}{\beta_c c} \right] \quad , \tag{3-1-20}$$

the transfer function is reduced to

$$G = \frac{z_c}{j}\frac{z_d}{A}(1 - \cos A - j\sin A) \quad , \tag{3-1-21}$$

then the total gain $|G|$ is given by

$$|G| = |Z_c| \cdot \frac{z_d}{A} 2\sin\frac{A}{2} \quad . \tag{3-1-22}$$

3-2. The Parameters and the Performance of the T.W. Helix

The cross section of the beam is assumed with the aperture of the guard which keeps out the electrostatic position sensitive beam monitor from the direct bombardment of the beam and is the minimum aperture in the vacuum chambers of TARN. The area of the beam cross section 72 cm^2 , 18 cm in width and 4 cm in height. The radius of a circle of the same area is

$$a \sim [\ 72/\pi\ ]^{1/2} = 4.79 \text{ cm} \quad .$$

With this beam radius, and the pitch 1/n and the radius ℓ of the helix are calculated as follows.

Inductance L of the helix ; $L = \mu_0 S n^2 \eta$ (3-2-1)

$S = \pi \ell^2$; area of the cross section of the helix,

n ; turn number of the helix per unit length,

η ; Nagaoka factor,

Capacitance C of the helix ; $C = \dfrac{2\pi\varepsilon_0}{\ln \frac{b}{\ell}}$ (3-2-2)

b ; radius of the outer-conductor .

Then the characteristic impedance of the T.W. helix, Z_0 , is

$$Z_0 = [\ \frac{L}{C}\ ]^{1/2} \quad . \tag{3-2-3}$$

The phase velocity along the T.W. helix, v_p , must be agreed with the particle velocity βc ,

$$\frac{1}{v_p} = [\ LC\ ]^{1/2} = \frac{1}{\beta c} \tag{3-2-4}$$

and the pitch is agreed, too,

$$[\ c \frac{1/n}{\beta c}\ ]^2 = (\ \frac{1}{n}\ )^2 + (\ 2\pi\ell\ )^2 \quad . \tag{3-2-5}$$

With

$$\beta \sim 0.12 \quad ,$$

$$\frac{1}{\beta^2} >> 1 \quad ,$$

the pitch 1/n is given by

$$\frac{1}{n\beta} = 2\pi\ell \qquad (3\text{-}2\text{-}6)$$

Therefore,

$$\eta = \frac{Z_0 \cdot 4\pi\beta}{z_0} \qquad (3\text{-}2\text{-}7)$$

$$\ln \frac{b}{\ell} = \frac{2\pi Z_0 \beta}{z_0} \qquad (3\text{-}2\text{-}8)$$

where

$z_0 = [\frac{\varepsilon_0}{\mu_0}]$; characteristic impedance of the vacuum .

The typical parameter sets, which are appreciable to TARN, are calculated as shown in Table 3-1 with Eqs. (3-2-7) and (3-2-8). Because the beam radius a is set to 4.79 cm, value of γ_s is gained with x-value of the cross point of Fig. 3-2 ,

$$\gamma_s = \frac{x}{0.0479}$$

These values are defined each frequencies and the lowest γ_s , is shown in Fig. 3-3 . Among these values, the lowest γ_s is used in the calculation. With the second parameter set of Table 3-1, coupling impedance $|Z_c|$, total gain $|G|$ and radial electric field $E_z(r)$, are calculated with Eqs. (3-1-10), (3-1-21), (3-1-6) and (3-1-7) as shown in Figs. 3-4, 3-5 and 3-6, respectively. Because parameters of the helix are calculated in the assumed coaxial system, these parameters are modified to fit the rectangular aperture of the guard. In the modification, inductance of the helix L is proportional to cross section area

of the helix S, the area is conserved, and capacitance C is depended on radii of the helix and the outer-conductor (b and ℓ), the difference of these radii (b-ℓ) is conserved. Therefore the cross section of the helix is

5.7 cm height x 19.7 cm width ,

and that of the outer-conductor is

12.7 cm height x 26.7 cm width .

The total circumference length of the helix is 50.9 cm, and the pitch is 6.1 cm. The appreciable length of the T.W. helix chamber is 80 cm maximum, length of the helix is decided 70 cm as shown in Fig. 3-7 and the turn number is 11.5 turns. With Eq. (3-2-3) characteristic impedance of the T.W. helix is calculated to 230 Ω . To connect with a 50 Ω network system, one end is terminated with a 230 Ω metal film resistor, and the other one is output side which is taken the impedance transforming with 56 Ω and 200 Ω resistors as shown in Fig. 3-8. Some example of these connections are shown with the resistor sets in Figs. 3-9-a and -b. Up to about 200 MHz, the data which is shown as Fig. 3-9-b , is better than other ones as a whole, and these resistors are set in the beam pickup in the vacuum chamber to prevent the S/N ratio of the minute picked up signal wronger. At the kicker, the problem of impedance matching with power amplifier and the kicker is more important because that the rising time and the power efficiency are depended on connected device. However, the effect is expected to be small because that the impedance of the kicker is rather large than that of the power amplifier, the resistors are set out of the vacuum chamber.

4. Notch Filter [15]

Notch filter has notches at a fundamental and the harmonic frequencies and the phase of upper or lower of the notch frequencies is in turn at the center frequencies. The parameters of the notch filters are chosed to modify the picked up signal that make larger momentum correction the particles which are in longer from the center frequencies.

In the case of coaxial cable which has characteristic impedance Z_0 , length ℓ and load impedance Z_L at one end, the impedance Z_ℓ from the other end is,

$$\frac{Z_\ell}{Z_0} = \frac{Z_L + Z_0 \tanh(\gamma\ell)}{Z_0 + Z_L \tanh(\gamma\ell)} \quad . \tag{4-1}$$

$$(\gamma = \alpha + jk_z \ , \ k_z = \frac{2\pi}{\lambda})$$

In this equation with no loss cable ($\alpha=0$) and shorted at the end, $Z_L=0$, the impedance Z_ℓ is

$$Z_\ell = jZ_0 \tan(k_z\ell) \quad . \tag{4-2}$$

Notch frequencies are those where amplitude of the impedance $|Z_\ell|$ has the maximum values,

$$k_z\ell = n\pi \tag{4-3}$$

Then, the length of the notch filter is a half of the wave length of fundamental frequency of the coaxial cable with a shorted end.

4-1. Coaxial Cable for Notch Filter

As loss of coaxial cable decides depth of dip in amplitude of notch filter, the frequency dependence of the depth at the notch center and pole frequencies is calculated in the short end notch filter ($Z_L = 0$). In this case, $e^{ikz\ell} = 1$ at notch center frequencies, and $e^{ikz\ell} = -1$ at notch pole frequencies. As the fundamental frequency of the notch filter under consideration is about 1.1 MHz, the difference of the center and pole frequencies is about 550 kHz. For simplicity, the loss factor is assumed to be constant over 550 kHz, the gain difference at adjacent center and pole frequencies is

$$\frac{|Z_\ell(\text{pole})|}{|Z_\ell(\text{center})|} = \frac{(e^{-2\alpha\ell} + 1)^2}{(e^{-2\alpha\ell} - 1)^2} = \coth^2(\alpha\ell) \quad . \qquad (4\text{-}1\text{-}1)$$

In the Eq. (4-1-1), the gain difference of the notch center and pole frequencies is increased as absolute value of cable loss is increased the cable loss is increased. Therefore a coaxial cable of low loss factor is preferable for a notch filter. The losses of some easily and commercially available coaxial cables are shown in Fig. 4-1. The length of the coaxial cable as the notch filter is written as

$$\ell = \frac{n\lambda}{2} = \frac{1}{2} n \frac{c}{f_0} \qquad (4\text{-}1\text{-}2)$$

where,

n ; wave shortened ratio = 1 (100 %)

λ ; wave length

f_0 ; fundamental frequency = 1.1 MHz

c ; light velocity ,

then the length is about 136 m . A flexible type cable wound on to a drum is chosen rather than a straight type at the cost of loss factor. Thus HF-coaxial cable series made by Hitachi Cable, Ltd. is chosen, and the performances of some examples of these cables are listed in Table 4-1, and the last column shows the cable lengthes for the fundamental frequency 1.10 MHz and 1.14 MHz, respectively. And the frequency dependences of these cables' impedances at the center and pole frequencies with short end for the fundamental frequency 1.10 MHz are written as

$$\text{center gain} \quad ; \quad A = \frac{|Z_\ell|}{|Z_0|} = \frac{1 - 10^{-2\alpha\ell/20}}{1 + 10^{-2\alpha\ell/20}} \qquad (4\text{-}1\text{-}3)$$

$$\text{pole gain} \quad ; \quad A = \frac{|Z_\ell|}{|Z_0|} = \frac{1 + 10^{-2\alpha\ell/20}}{1 - 10^{-2\alpha\ell/20}} \quad . \qquad (4\text{-}1\text{-}4)$$

The impedances at the center in dB are shown in Fig. 4-2. In these cables, HF-39Γ coaxial cable is chosen for the momentum cooling experiment at TARN and the cable length is determined to 119.66 m for the fundamental frequency 1.14 MHz, and a 4.35 m cable is added for the fundamental frequency 1.10 MHz. This cable length were decided with the measurement of the phase of the frequency 1.10 MHz and 1.14 MHz by Hitachi Cable, Ltd. and the common differences are fallen into $-0.3^\circ \sim 0^\circ$, i.e. -20 cm ∿ 0 cm in length. A coaxial trombone tuner (Nihon Koshuha Co., Model SRC-S-222P) is attached to the end of the cable as a fine tuner from 0 cm through 40 cm. The other end of this tuner is terminated with an open or short terminator (WILTRON, Model 22N50) .

4-2. Resistor-dependence

The shape and depth of notch gain depends on the resistor values attached at the ends of the filter [15] . The values of the gain are calculated with the 4 element analysis [16] .

Load impedance of the cable Z_ℓ and resistors R_S are defined as in Fig. 4-2. Then,

$$\begin{pmatrix} V_1 \\ I_1 \end{pmatrix} = \begin{pmatrix} 1+\frac{R_S}{Z_\ell} & \frac{2R_SZ_\ell + R_S^2}{Z_\ell} \\ \frac{1}{Z_\ell} & 1+\frac{R_S}{Z_\ell} \end{pmatrix} \begin{pmatrix} 1 & 0 \\ \frac{1}{R} & 1 \end{pmatrix} \begin{pmatrix} V_2 \\ I_2 \end{pmatrix}$$

$\therefore$)

$$\begin{pmatrix} V_1 \\ I_1 \end{pmatrix} = \begin{pmatrix} 1+\frac{R_S}{Z_\ell} + \frac{2R_SZ_\ell + R_S^2}{Z_\ell R} & \frac{2R_SZ_\ell + R_S^2}{Z_\ell} \\ \frac{1}{Z_\ell} + \frac{1}{R}\left(1+\frac{R_S}{Z_\ell}\right) & 1+\frac{R_S}{Z_\ell} \end{pmatrix} \begin{pmatrix} V_2 \\ I_2 \end{pmatrix} \quad . \qquad (4\text{-}2\text{-}1)$$

In this Eq. (4-2-1), with $I_2 = 0$

$$\frac{V_1}{V_2} = 1 + \frac{R_S}{Z_\ell} + \frac{2R_SZ_\ell + R_S^2}{Z_\ell R}$$

$$= \frac{R_S(R + R_S) + (R + 2R_S)Z_\ell}{Z_\ell R} \quad . \qquad (4\text{-}2\text{-}2)$$

Thus the voltage gain of this filter is,

$$\frac{V_1}{V_2} = \frac{Z_\ell R}{R_S(R + R_S) + (R + 2R_S)Z_\ell} \quad , \qquad (4\text{-}2\text{-}3)$$

where Z_ℓ is

$$Z_\ell = Z_\ell^S = Z_0 \tanh(\gamma\ell) \qquad ; \quad \text{short end} \qquad (4\text{-}2\text{-}4)$$

or

$$Z_\ell = Z_\ell^0 = Z_0 \coth(\gamma\ell) \quad ; \text{ open end} \quad . \tag{4-2-5}$$

For the resistors of R_S = 50 Ω, 100 Ω, 200 Ω, 400 Ω, and 600 Ω, the gains of the notch filter with HF-39D cable at the neighborhood of the 30-th harmonics are calculated and shown in Fig. 4-4 on the assumption the cable losses are negligible for simplicity.

In the same way, the 4-element representation of the short end notch filter added to the same one as in Fig. 4-5 is

$$\begin{pmatrix} V_1 \\ I_1 \end{pmatrix} = \begin{pmatrix} 1+\frac{R_{S1}}{Z_{\ell 1}} + \frac{2R_{S1}Z_{\ell 1}+R_{S1}^2}{Z_{\ell 1}R} & \frac{2R_{S1}Z_{\ell 1}+R_{S1}^2}{Z_{\ell 1}} \\ \frac{1}{Z_{\ell 1}} + (1+\frac{R_{S1}}{Z_{\ell 1}})\frac{1}{R} & 1+\frac{R_{S1}}{Z_{\ell 1}} \end{pmatrix} \tag{4-2-6}$$

$$\times \begin{pmatrix} 1+\frac{R_{S2}}{Z_{\ell 2}} + \frac{2R_{S2}Z_{\ell 2}+R_{S2}^2}{Z_{\ell 2}R} & \frac{2R_{S2}Z_{\ell 2}+R_{S2}^2}{Z_{\ell 2}} \\ \frac{1}{Z_{\ell 2}} + (1+\frac{R_{S2}}{Z_{\ell 2}})\frac{1}{R} & 1+\frac{R_{S2}}{Z_{\ell 2}} \end{pmatrix} \begin{pmatrix} V_2 \\ I_2 \end{pmatrix}$$

then

$$\frac{V_1}{V_2} = \left[1+\frac{R_S}{Z_\ell} + \frac{2R_SZ_\ell+R_S^2}{Z_\ell R} \right]^2 + \frac{2R_SZ_\ell+R_S^2}{Z_\ell}\left[\frac{1}{Z_\ell} + (1+\frac{R_S}{Z_\ell})\frac{1}{R} \right] \quad . \tag{4-2-7}$$

And the representation of the short notch filter added to the open one is obtained by replacing Eq. (4-2-4) by Eq. (4-2-5) in Eq. (4-2-6) and (4-2-7). Thus

$$\frac{V_1}{V_2} = \left(1+\frac{R_S}{Z_\ell^S} + \frac{2R_SZ_\ell^S+R_S^2}{Z_\ell^S R} \right)\left(1+\frac{R_S}{Z_\ell^0} + \frac{2R_SZ_\ell^0+R_S^2}{Z_\ell^0 R} \right)$$

$$+ \frac{2R_SZ_\ell^S+R_S^2}{Z_\ell^S}\left[\frac{1}{Z_\ell^0} + (1+\frac{R_S}{Z_\ell^0})\frac{1}{R} \right] \quad . \tag{4-2-8}$$

The absolute values of Eqs. (4-2-7) and (4-2-8) show the notch gain, and are shown in Figs. (4-6) and (4-7), respectively. The typical examples of the gain and phase of the notch filters were measured in frequency domain with a spectrum analyzer TR-4172 (Takeda Riken Industry Co., Ltd.) and shown in Fig. 4-8 .

5. Effect of Notch Gain Shape on the Beam Distribution

In this chapter, beam distribution which is changed by the momentum correction with the cooling system is calculated in very simple case with two typical notch filters.

For simplicity,

1) the maximum gain of the notch filter is 50 V and particles are given correction energy according to those gains.

2) there is no noise at all.

3) particles are accelerated in lower side of the notch center frequency and decelerated in higher.

4) only 1 band is considered.

(fundamental frequency ; 1.1 MHz, 30-th harmonic band)

Notch gain y is defined as

$$y = G(f) \qquad (5\text{-}1)$$

and voltage gain is 50 volt at 33.55 MHz, voltage gain at f MHz is

$$50 \times G(f) \quad .$$

By the assumptions, the energy gain ΔE is $50 \times G(f)$ eV. Frequency difference is given by

$$\frac{\Delta f}{f} = \frac{3}{4}\frac{\Delta p}{p} \quad , \tag{5-2}$$

as

$$\frac{\Delta p}{p} = \frac{1}{2}\frac{\Delta E}{E} \tag{5-3}$$

and

$$\frac{\Delta f}{f} = \left(\frac{1}{\gamma^2} - \frac{1}{\gamma_{tr}^2} \right) \frac{\Delta p}{p} \quad , \tag{5-4}$$

where

$$\frac{1}{\gamma^2} - \frac{1}{\gamma_{tr}^2} = \frac{3}{4} \quad .$$

Then

$$E = A\, f^{3/8} \tag{5-5}$$

and in the case of f=33.00 MHz with E=8.0 MeV

$$E = 8.0 \times \left(\frac{f}{33.00} \right)^{8/3} \quad . \tag{5-6}$$

Frequency change is reduced to

$$\Delta f = \frac{3}{4}\frac{1}{2}\frac{\Delta E}{E} f \quad , \tag{5-7}$$

and the energy of the particle E_s is

$$E_s = 8.0 \times \left(\frac{f_s}{33.00} \right)^{8/3} \quad , \tag{5-8}$$

where

$$f_s = f - \Delta f \quad . \tag{5-9}$$

Consider two typical notch filters that have simple gains vs. frequency and their shapes are really similar to real notch filters with resistors R_s = 50 Ω or 600 Ω , respectively, as shown in Fig. 5-1. The frequency distribution of the single particle beam is varied with the correction ΔE. The variations

are calculated using above equations, and the result is shown in Fig. 5-2. In Fig. 5-2, at the beginning stage in case A, the particles far from the center of the frequency distribution are moved to the center faster, and those near the center are very slowly. In case B, all particles of frequency distribution are moved faster and the cooling time is shorter, but the final distribution is wider. So, the selection of R_s value effects on the cooling time and the width of the final distribution, and we must select R_s with caution. In the first trial of TARN cooling experiment, R_s will be selected to 50 Ω and the notch gain will be similar to that in case B.

6. Network [17]

Revolution frequency of the particles is 1.1 MHz and the revolution time is 0.88 μsec. Typical rising time of the preamplifiers is a few nsec and the delay time is the same order, all combinations of straight sections of TARN for the beam signal pickup and the kicker are possible. In easier selection, S4 and S7 of the straight sections are used for momentum cooling experiment at TARN. The particles move in 0.33 μsec between the two sections, and the delay time of the feedback system for the experiment is fitted the time.

As shown in Fig. 6-1, the picked up signal of the beam is amplified by the TRONTECH pre-amplifier which has 60 dB gain and 1.5 dB noise figure and has frequency range from 5 MHz to 500 MHz

at the first stage. Next stage, the signal is amplified by the TRONTECH pre-amplifier and attenuated down to the appreciate amplitude into pass-band filters. These pass-band filters pass the component of the modified signal. The 4-th stage, the signal is passed through the appreciate length coaxial line 5D4E in order to adjust the delay time and taken into the 50 Watt. wide band power amplifier. At the last stage, the output power of the power amplifier is introduced into the kicker and the particles are corrected. Gain and phase vs. frequency of the TRONTECH pre-amplifier was measured and the performance of the pre-amplifier is plenty up to about 200 MHz. Attenuators are programmable step ones, Weinschel Engineering, Model No. 3200-2, and the smallest step is 0.25 dB, the maximum 63.75 dB. The delay time is not changed when the attenuation value is changed and the typical time is shown in Table 6-1.

Coaxial switch (TRANSCO PRODUCTS, Model No.919C70100) is used for check of the system and the loss vs. frequency of the switch is shown in Fig. 6-2.

The attenuation and coaxial switch are regulated remotely from the control room of TARN.

To make coincidence the picked up signal with the particles, delay times of network elements were measured with the circuit shown in Fig. 6-3, and the total delay time was 24 nsec. As the time of flight of the particle between the pick-up and the kicker is 0.34 μsec when the revolution frequency is 1.10MHz, the 66.1 m 5D4E coaxial cable is used as a delay line. A trombone tuner is attached for fine tuning in range of 1 nsec. Typical values of the measured delay times of elements are listed in

Table 6-1.

7. Data Taking System

The process of the momentum cooling at TARN is observed as the variation of the distribution of the beam revolution frequency. The output signal of the first stage pre-amplifier is divided by Power Splitter (HP, Model 11549A), is observed with a spectrum analyzer. Multiturn injected beam, rf stacked beam or multiturn injected and rf stacked beam is selected as the momentum cooling experiment at TARN. Data taking system must be possible to measure the cooling effect in all cases, but the cooling times and the signal to noise rate of beams are very different, as the momentum spreads, the intensities etc. are very different. The data taking system is required to meet various use of the sensitivity, stability, measuring time and memory capacity. To satisfy these points, the data taking system is composed of a spectrum analyzer and a microcomputer which works not only as an external memory but also as a controller of the experimental period and time schedule.

7-1. Spectrum Analyzer

Some indispensable performances of spectrum analyzer for the experiment, are described as under,

1) Long time range frequency stability.

This means that the cooling time is expected about one minute, and it's value will be longer about 10 times under some conditions. These experiments require about 10 times long range measurement of half-life of transient phenomena. And at the initial stage of the experiment averaging measurement is an useful method, because the S/N ratio is expected to be poor as above.

2) It is better as the measuring time is shorter.

But it is essentially decided with the characteristics of the filter which is used to analyse signals, and related with scan width and frequency resolution band width.

3) Data transfer time is hoped to be shorter than the measurement time.

To achieve the transfer time shorter, the spectrum analyzer must have parallel data I/O and must change the data bit patterns. This means that the spectrum analyzer is an intelligent type which is controlled by CPU and the internal program.

Then TR-4172 (Takeda Riken Industry Co., Ltd.) is chosen as the spectrum analyzer which satisfies these specifications, and its performance is described in Table 7-1. Takeda Riken Industry Co., Ltd. was requested to improve the spectrum analyzer in two points, and they achieved by rewriting the ROM in the spectrum analyzer. One of the requests is to exchange movable averaging for simple averaging, and so averaging of the data is not carried out on real time. With this modification, the time costed to calculate the average is only time for a simple division. The other is data transfer in binary code in stead of

the one in ASCII code in GP-IB bus. In usual usage data bit patterns are in binary code at the first stage of spectrum measurement with the spectrum analyzer and then transformed to ASCII code. In this modification the initial data bit patterns in binary code is kept. The length of one datum is about 10 times shorter than that in ASCII code. Processing time is reduced, as the time for transforming the data code is free.

7-2. Computer

At the beginning of designing the equipments for the momentum cooling experiment at TARN, the computer was imaged to be only an external large memory. We chose once a usual personal computer with Z80 CPU of 4 MHz clock, which has two 5" floppy disk drivers and GP-IB bus as data transfer line with ASCII code, and the program is written with BASIC interpriter. The data reading time into the computer was measured with this system. To measure the reading time only, the circuit which makes DAV status with NDAC and NFRD state directly by using fast TTL IC was composed as in Fig. 7-1, which was free from the response time with external equipment. TTL IC's in the circuit have faster active time than 10 nsec, the time in this circuit is negligible. This result is shown in Fig. 7-2, and the reading time per datum is 410 μsec. As one spectrum (= 1 kB) is composed of 500 data, the reading time per 1 spectrum is

410 μsec x 500 data = 200 msec .

Moreover we must consider the writing time of these data onto the floppy disk, then it takes about 10 sec to transfer data from the spectrum analyzer, read into CPU, and write on a floppy disk. Thus the data transfer must be acted in Direct Memory Access mode to reduce this time.

From this reason the computer was decided on a microcomputer THE BOX (ZAX Co.) and the application program was made by SYST Co., Ltd. The performance of THE BOX is listed in Table 7-2, and the flow chart of the program is shown in Fig.7-3.

This data taking system can achieve a shorter than 1 sec measurement time repeat measurements about 1000 times, under the condition of a 30 MHz center frequency, 1MHz span width, 3 kHz resolution band width, 8 times averaging of 500 points data, i.e. 1 kB per spectrum. The items of the measurement process are as follows ;

measurement of a spectrum	;	40 msec,
averaging	;	20 msec,
preparing data transfer through GP-IB bus	;	25 msec,
reading data into CPU	;	40 msec,
writing data onto a floppy disk	;	167 msec,
total		200 msec.

To know the content of the repeating time, the data reading time and the interval between the measurement with the spectrum analyzer and writing data on the floppy disk were measured. Two STROBE signals were made before and after data reading by CPU, and the intervals between the two signals measured 39$\pm$1 msec/kB. Next, STROBE signals were made after finishing of data reading by CPU, and the operation of this system was repeated to the time

schedule shown in Fig. 7-4. The interval between the STROBE signals measured 167±10 msec . In the same conditions, 1 cycle time of the measurement repeated to the time schedule shown in Fig. 7-5 is expected to be about 1400 msec .

Acknowledgements ;

We wish to thank Profs. Y. Hirao and T. Katayama and all members of NUMATRON working group, they gave us the chance to try the momentum cooling experiment at TARN. And it is a pleasure to thank Prof. K. Hushimi and Dr. H. Eickhoff for consulting us about the calculation of the radial electric field made by the beam column of the T.W. helix coupler , Drs. S. Yamada and T. Murakami for discussing the momentum cooling experiment with us, and Mr. K. Omata and Dr. H. Nishimura for advising us about the microcomputer of the data taking system. In this work, we had calculated the parameters of all equipments of this system with the calculators and after making orders of these parts we calculated once more the parameters with the M-180 IIAD computer of the computer center at INS.

References ;

[1] T. Katayama et al., INS report, NUMA-Report 17, 1980.

[2] H. G. Hereward, CERN 77-13, 1977.

[3] F. Sacherer, CERN-ISR-TH/78-11, 1978.

[4] D. Möhl et al., CERN/PS/AA 79-23, 1979.

[5] D. Möhl et al., Phys. Reports 58(1980) 73.

[6] G. Carron et al., Phys. Lett. 77B(1978)353.

[7] F. T. Cole and F. E. Mills, Ann. Rev. Nucl. Part. Sci. 31(1981)295.

[8] W. Kells, IEEE Trans. Nucl. Sci. NS-28(1981)2459.

[9] G. R. Lambertson et al., IEEE Trans. Nucl. Sci. NS-28 (1981)2471.

[10] W. Flood, LBL report, BECON-8 1/15/80, 1980.

[11] A. H. W. Beck et al., " SPACE-CHARGE WAVES And Slow Electromagnetic Wave ", Pergamon press, 1958.

[12] C. C. Johnson, IRE Trans. on Electron Devices (1959)189.

[13] D. M. Lee et al., Nucl. Instr. Meth. 109(1973)421.

[14] S. Sensiper, Proceedings of the I.R.E. (1955)149.

[15] G. Carron and L. Thorndahl, CERN-ISR-RF/78-12.

[16] K. Shimoda, " Erekutoronikusu no Kiso ", Shokabo (in Japanese).

[17] B. Leskovar and C. C. Lo, IEEE Trans. Nucl. Sci. NS-27 (1980)292.

Figure Captions ;

Fig. 2-1 ; Momentum Cooling Rate.

The curves which have G values are calculated with Eq. (2-1-9) in the case of $h_0 \gg 1$, and the other is calculated with Eq. (2-1-13).

Fig. 2-2 ; Vertical Betatron Oscillation Blow-Up.

Each curve is calculated with Eq. (2-3-10) in the case of $h_0 = 10$ and $G = 1$, and $Z_0/p_0 = 0.03$, 0.02 and 0.0075, respectively.

Fig. 2-3 ; Horizontal Betatron Oscillation Blow-Up.

The curves are calculated with Eq. (2-3-13) under the condition that $h_0 = 10$, $Z_0/p_0 = 0.0075$, $E_0 = 80$ mm·mrad, $\gamma = 1.14\ m^{-1}$ and $\eta = 1.2$ m and $G = 1$, 0.3, 0.1 and 0.03, respectively. The other one is calculated with Eq. (2-3-15).

Fig. 3-1 ; Parameters of the Travelling Wave Helix Coupler for calculating the Total Gain.

1) Outer-Conductor, 2) Helix, 3) Beam Column, z_c ; pitch of T.W. Helix, z_d ; Coupler length.

Fig. 3-2 ; Search for γ_s Values with the Frequencies.

The cross points of the two curves show the solutions of Eq. (3-1-5), and the x-value at the point is reduced to γ_s-value for each frequency.

Fig. 3-3 ; The Lowest γ_s to Frequency.

Fig. 3-4 ; Coupling Impedance $|Z_c|$.

Fig. 3-5 ; Total Gain $|G|$.

Fig. 3-6 ; Radial Electric Field $E_z(r)$.

Fig. 3-7 ; Drawing of 11.5 Turn T.W. Helix Coupler.
1) Pedestal Frange and Beam Guard made of 6 mm thick stainless steel, 2) Feedthrough : SMA-F-R, 3) Insulators which support the T.W. helix made of MACOOR, 4) Helix Tape of 10 mm width, 0.1 mm thick stainless steel, 5) Supporter made of ϕ 12 mm stainless steel rod, 6) M2 screw made of stainless steel, 7) Outer-Conductor made of 1 mm thick stainless steel plate.

Fig. 3-8 ; Chart and Calculation for Impedance Matching.

Fig. 3-9-a ; Test Circuit for Performance of T.W. Helix and Output Amplitude vs. Frequency.
in the case of no impedance matching.

Fig. 3-9-b ; Test Circuit for Performance of T.W. Helix and Output Amplitude vs. Frequency in the case of impedance matching.

Fig. 4-1 ; Losses of Some Coaxial Cables.

Fig. 4-2 ; Impedance at the Center Frequencies with Eq. (4-1-3).

Fig. 4-3 ; Notch Filter (I).
Amplitude and Phase of the Single Notch Filter depend on R_s-resistors values.

Fig. 4-4 ; Amplitude and Phase of Notch Filter (I).
R_s -dependence is calculated and R_s-values are shown in this figure.

Fig. 4-5 ; Notch Filter (II).
This one is composed of two single notch filters.

Fig. 4-6 ; Short End and Short End Notch Filter (II).

Amplitude and phase of the filter is calculated with some R_S -values and the values are shown in the figure.

Fig. 4-7 ; Short End and Open End Notch Filter (II) . (calculation)

Fig. 4-8 ; Single Short End Notch Filter.
R_S = 100 Ω .

Fig. 5-1 ; Typical Notch Filters for the Calculation.
Case A : similar to the notch filter with R_S = 600 Ω,
Case B : similar to the notch filter with R_S = 50 Ω.

Fig. 5-2 ; Variations of the Frequency Distributions.
Case A : with R_S = 600 Ω ,
Case B : with R_S = 50 Ω .

Fig. 6-1 ; Electrical Configuration of the Momentum Cooling.

Fig. 6-2 ; Loss vs. Frequency and Delay Time of the Coaxial Switch.
Top : Loss vs. Frequency ,
Bottom : Delay Time .

Fig. 6-3 ; Block Diagram of the Delay Time Measurement of Electrical Configuration.

Fig. 7-1 ; GP-IB Control Circuit for the Data Transfer Time.

Fig. 7-2 ; Data Transfer Time with GP-IB.

Fig. 7-3 ; Flow Chart of Application Program.

Fig. 7-4 ; Example of Time Schedule (I) of Data Taking for Momentum Cooling.

Fig. 7-5 ; Example of Time Schedule (II) of Data Taking for Momentum cooling.

Table Captions ;

Table 1 ; Parameter List of TARN for Proton Beam.

Table 3-1 ; Parameter List of T.W. Helix.

In the case that the radius of the helix is 6 cm.

η : Nagaoka factor, z_d : helix length in m,

Z_0 :impedance of the T.W. helix.

(The second set is that for 11.5 turn T.W. helix.)

Table 4-1 ; Parameter List of Some HF-Series Coaxial Cables.

Table 6-1 ; Delay Time of the Electrical Elements of the Momentum Cooling System.

Table 7-1 ; Specifications of the Spectrum Analyzer.

Referred to the Tentative Data Sheet written by Takeda Riken Industry Co., Ltd.

Table 7-2 ; Specifications of THE BOX.

Referred to the User's Mannual of THE BOX.

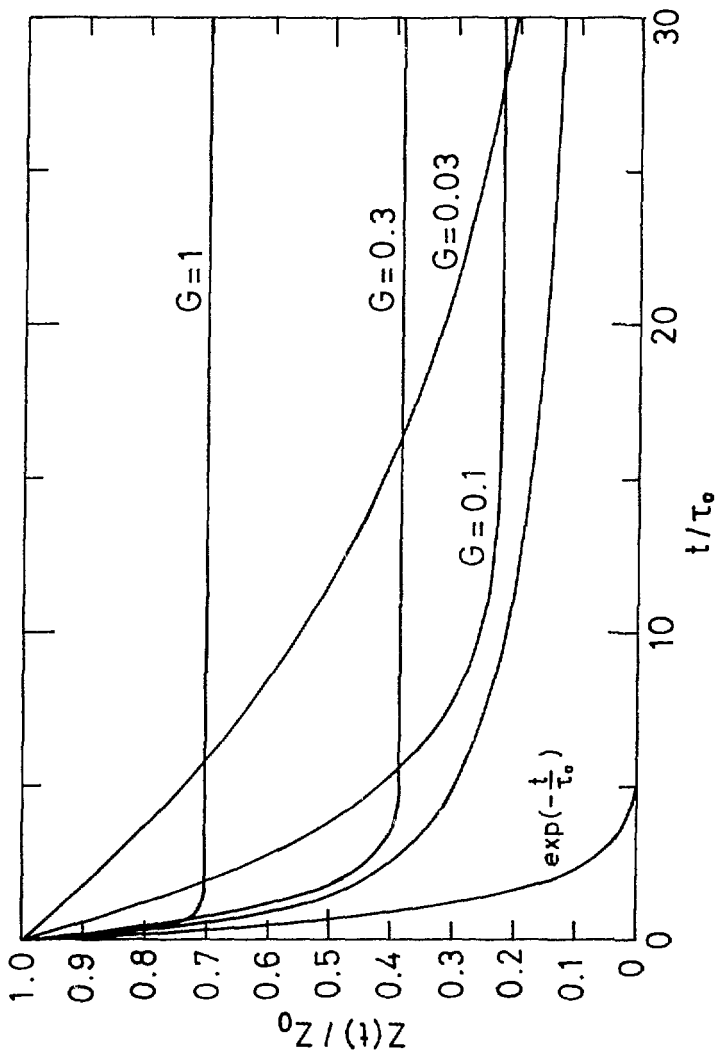
G=1
G=0.3
G=0.03
G=0.1
exp(-t/τ₀)
Z(t) / Z₀
t/τ₀
1.0
0.9
0.8
0.7
0.6
0.5
0.4
0.3
0.2
0.1
0
0
10
20
30

Fig. 2-1

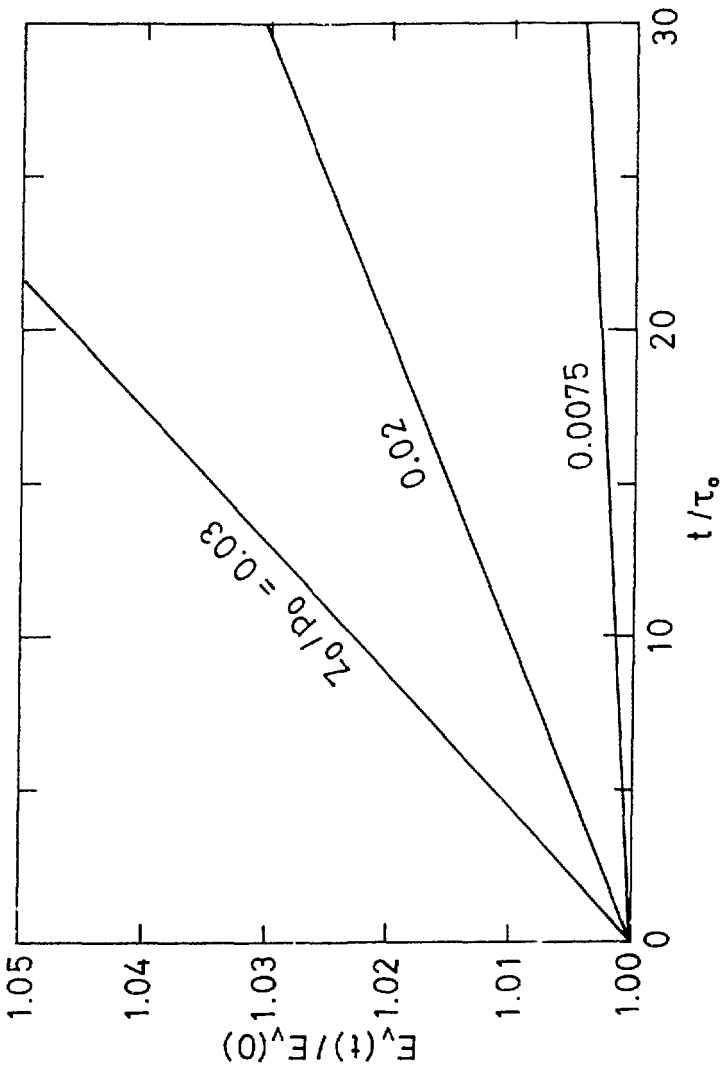
1.05
1.04
1.03
1.02
1.01
1.00
$E_v(t)/E_v(0)$
0
10
20
30
t/τ_o
$z_0/p_0 = 0.03$
0.02
0.0075

Fig. 2-2

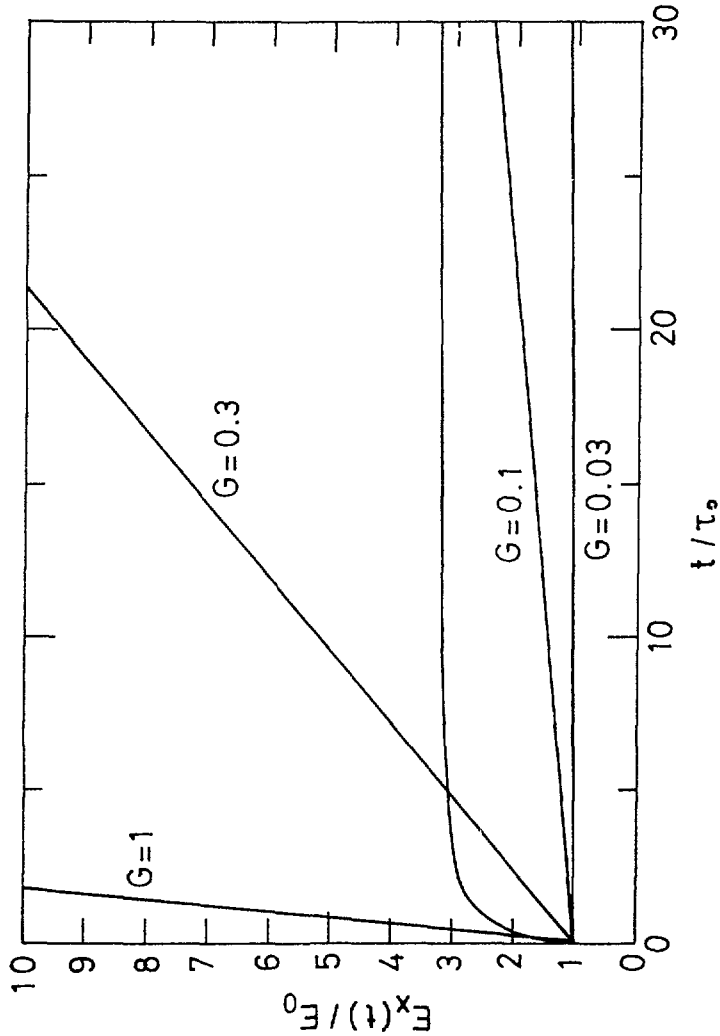

Fig. 2-3

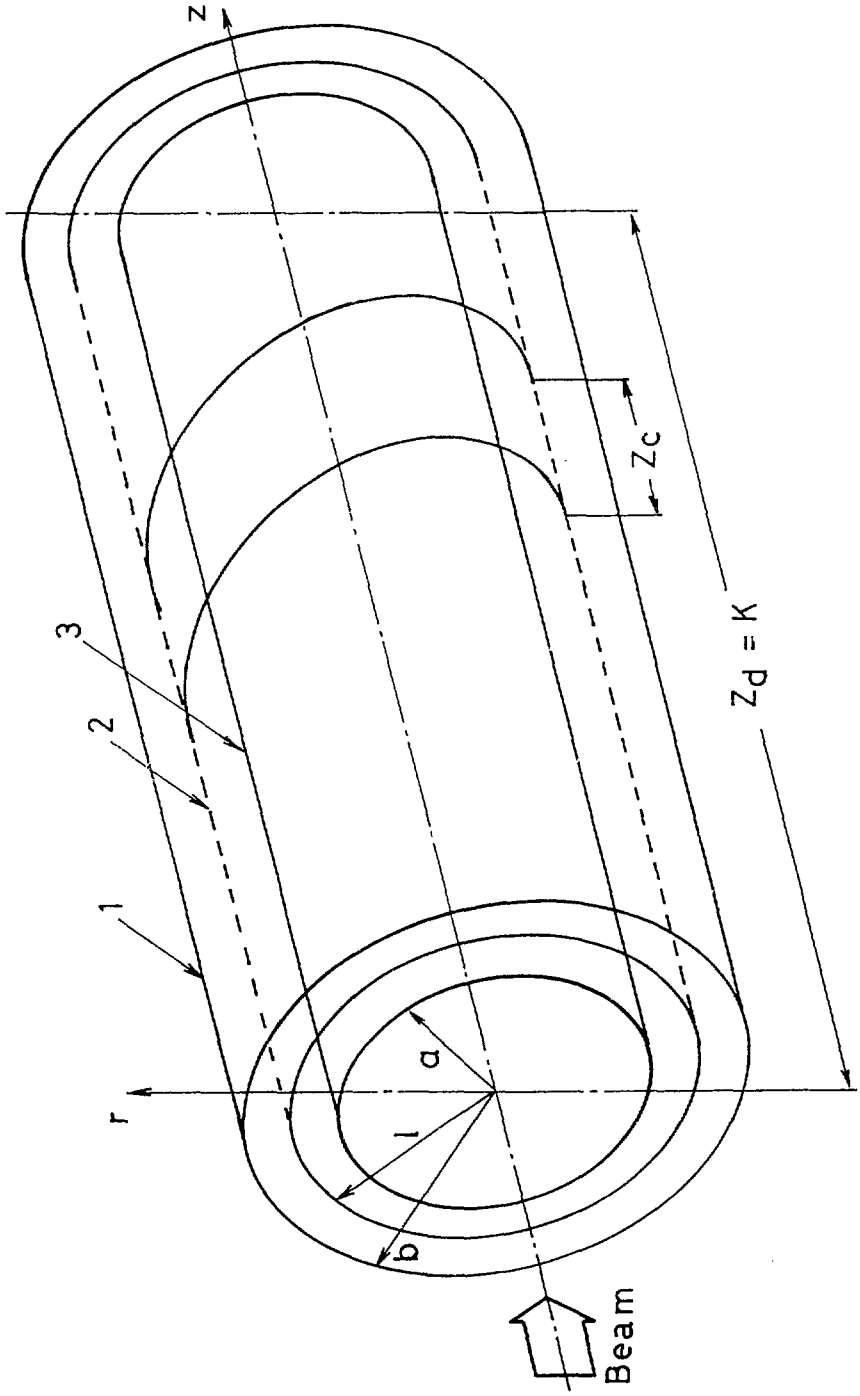

Fig. 3-1

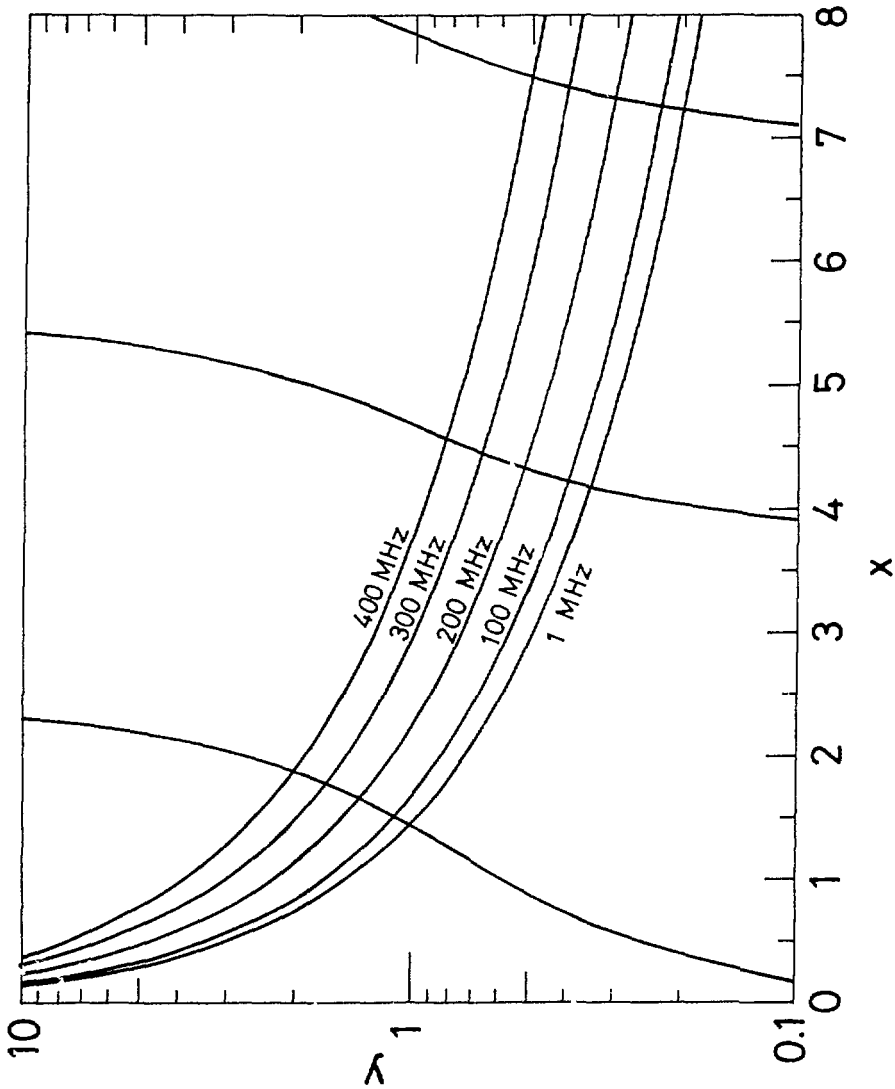

Fig. 3-2

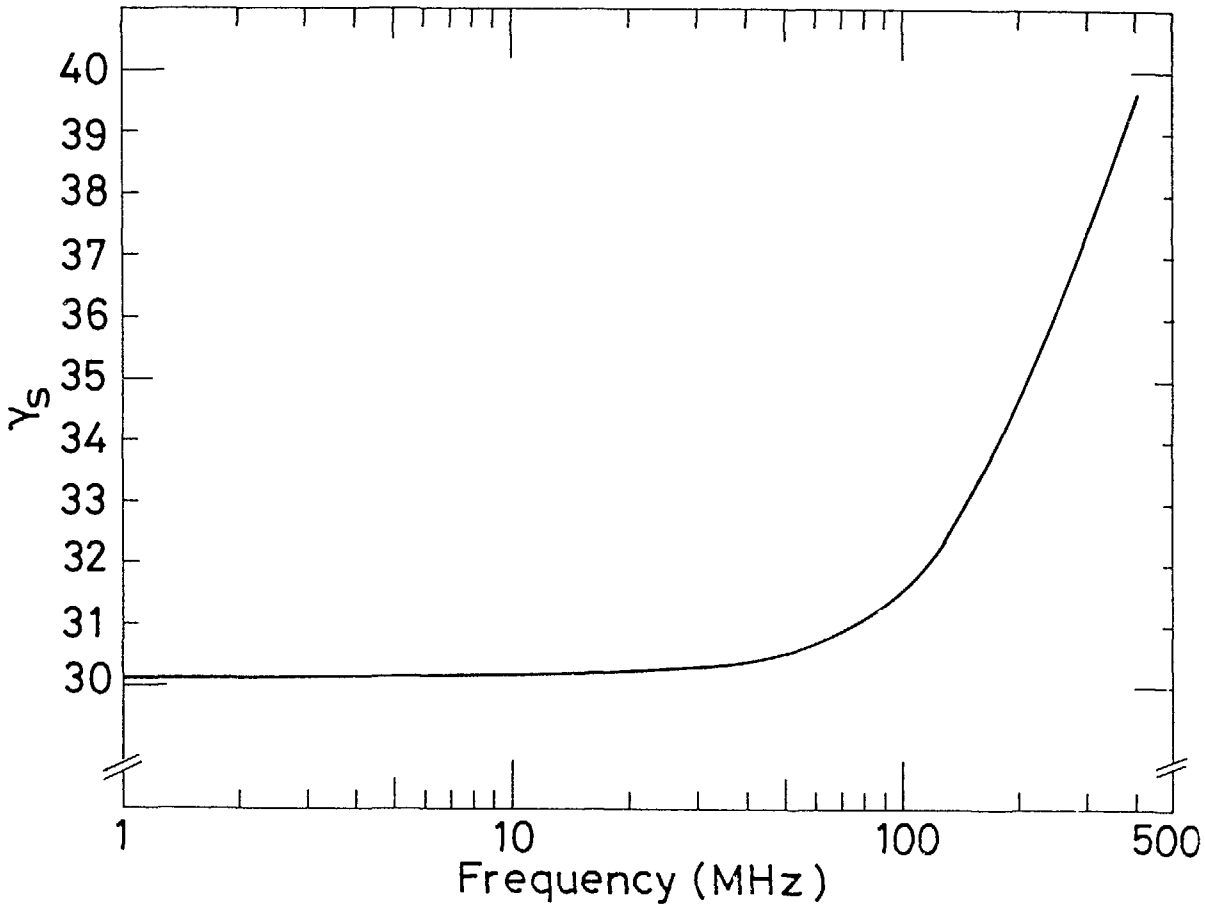

Fig. 3-3

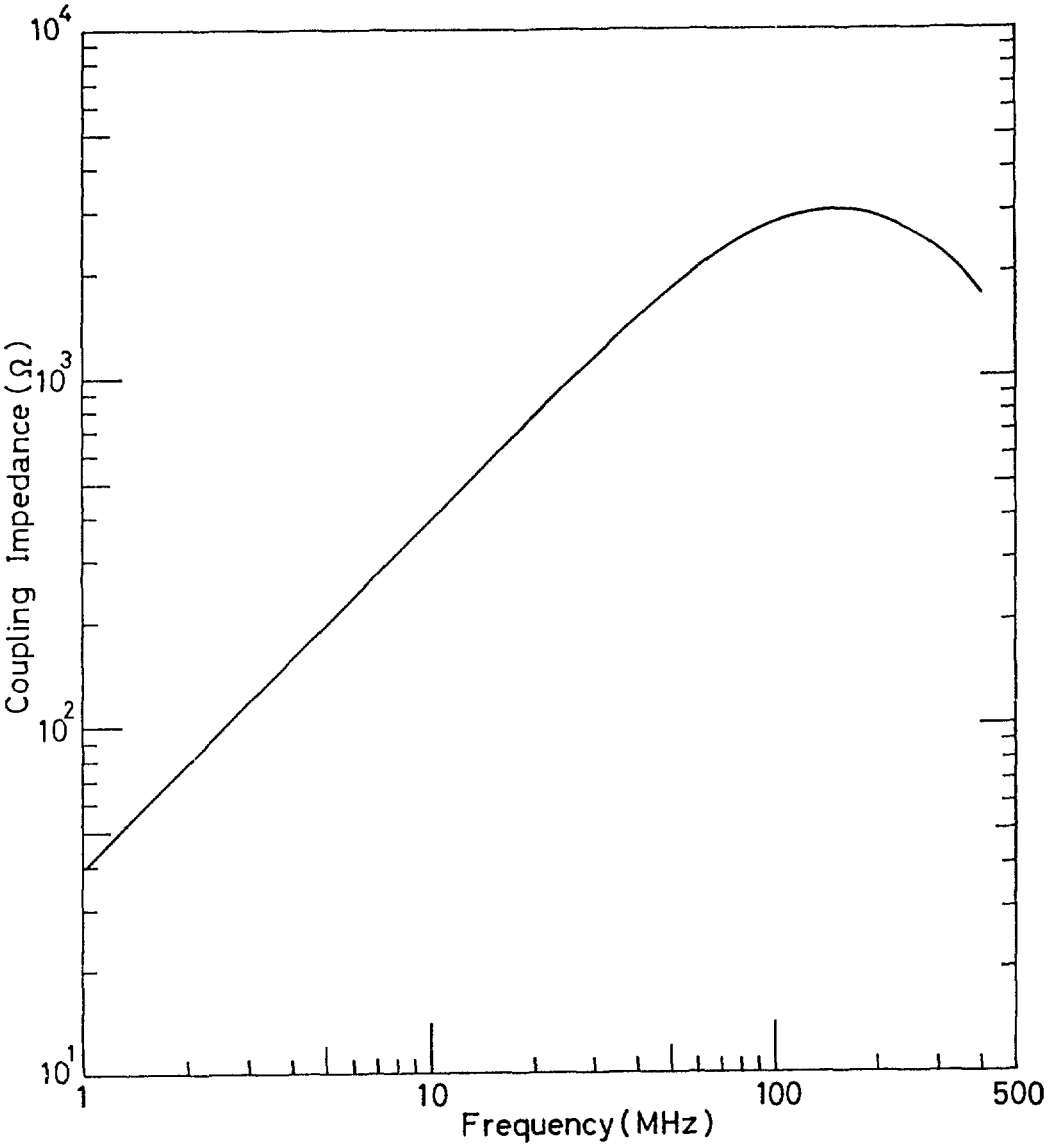
10^4
10^3
10^2
10^1
Coupling Impedance (Ω)
1
10
100
500
Frequency (MHz)

Fig. 3-4

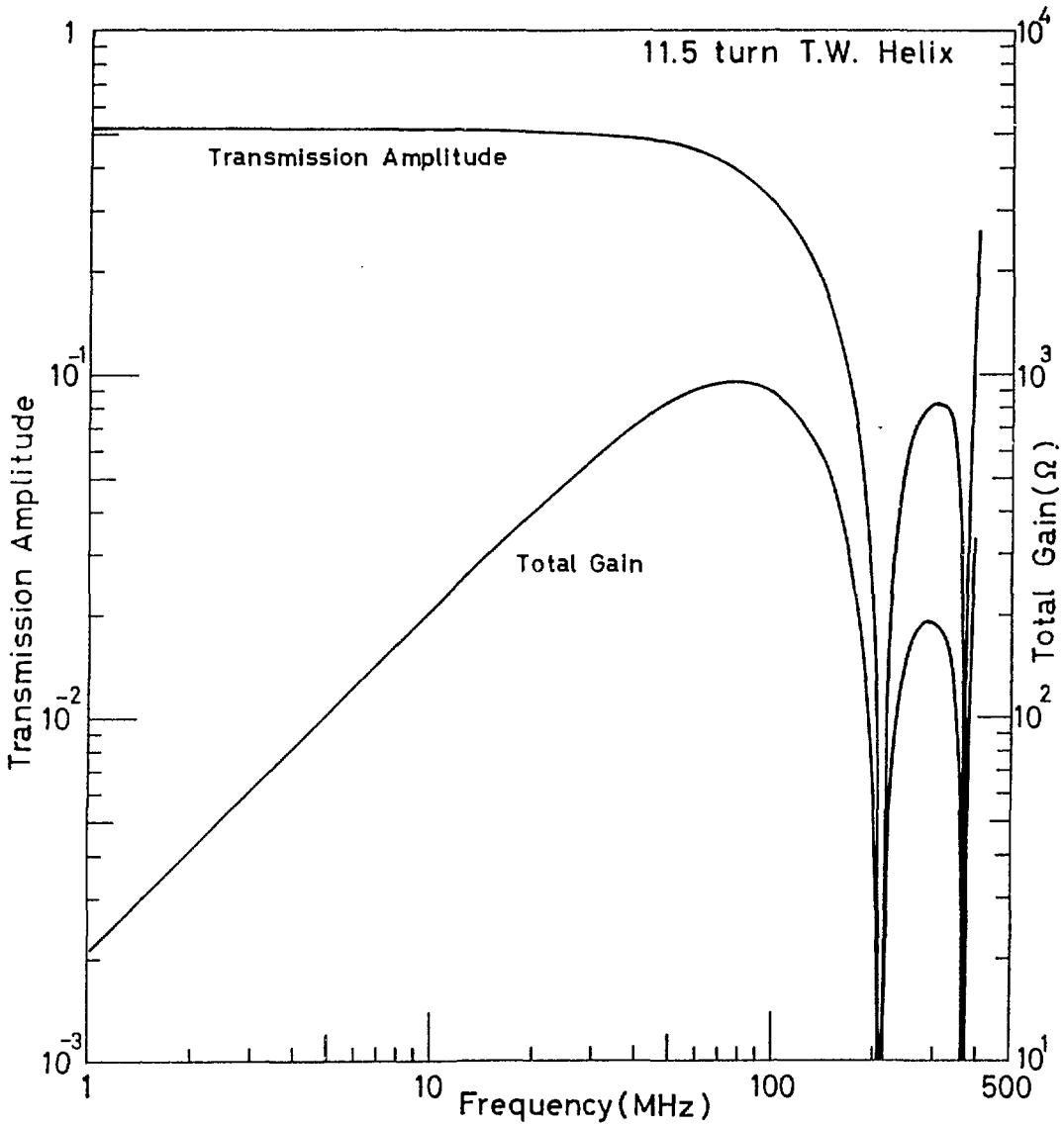
11.5 turn T.W. Helix
Transmission Amplitude
Total Gain
Transmission Amplitude
Total Gain(Ω)
Frequency(MHz)
1
10^{-1}
10^{-2}
10^{-3}
10^{4}
10^{3}
10^{2}
10^{1}
1
10
100
500

Fig. 3-5

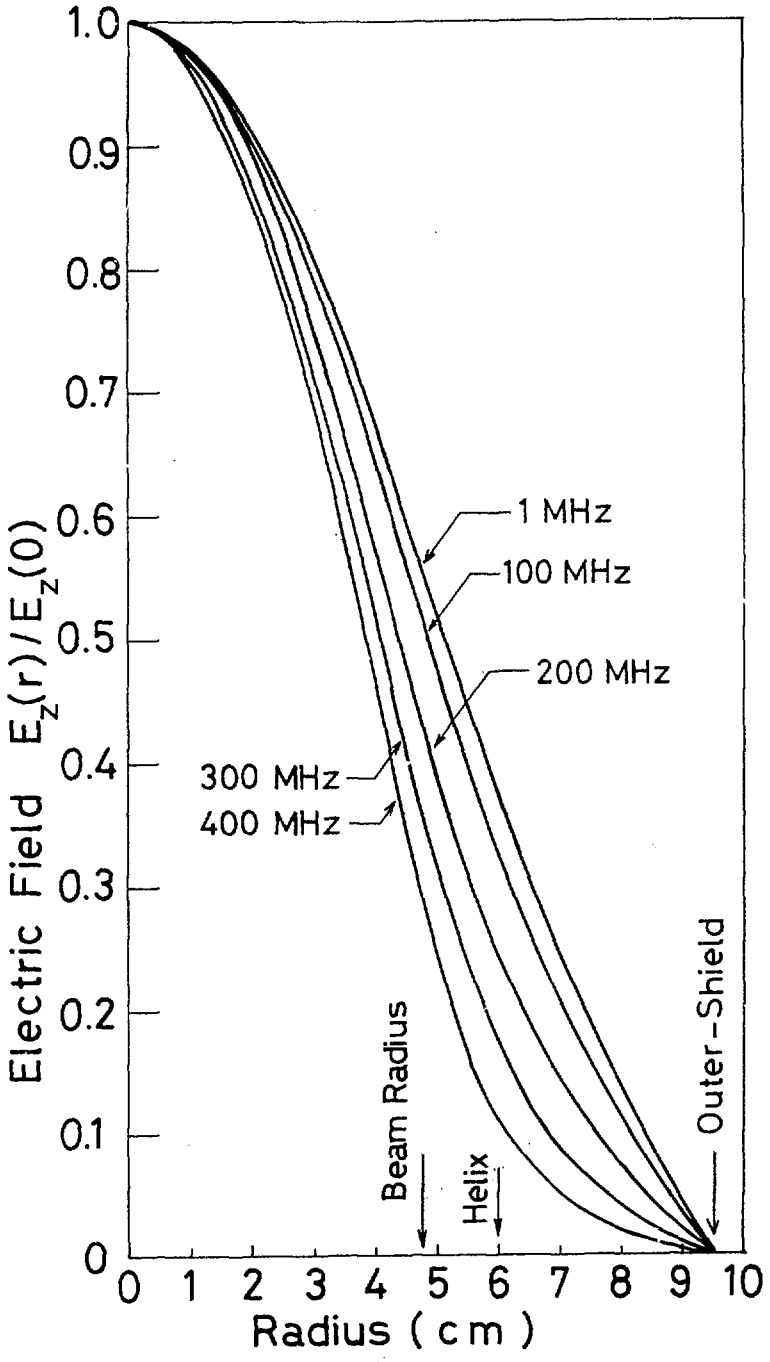
1.0
0.9
0.8
0.7
0.6
0.5
0.4
0.3
0.2
0.1
0
Electric Field $E_z(r)/E_z(0)$
0 1 2 3 4 5 6 7 8 9 10
Radius (cm)
1 MHz
100 MHz
200 MHz
300 MHz
400 MHz
Beam Radius
Helix
Outer-Shield

Fig. 3-6

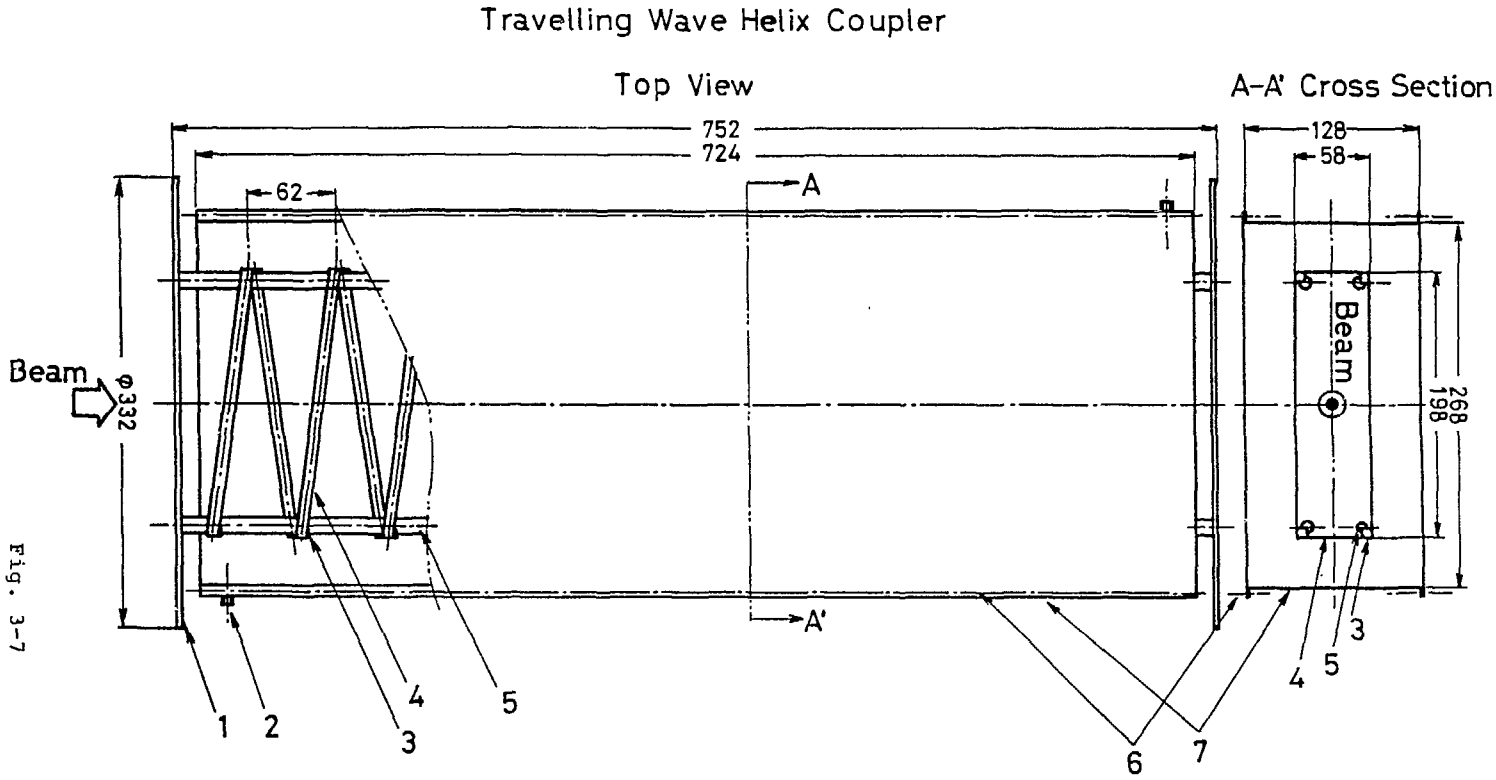
Travelling Wave Helix Coupler
Top View
A-A' Cross Section
752
724
62
A
A'
Beam
φ332
128
58
Beam
268
198
1
2
3
4
5
6
7
4
5
3

Fig. 3-7

Impedance Matching to 50 Ω

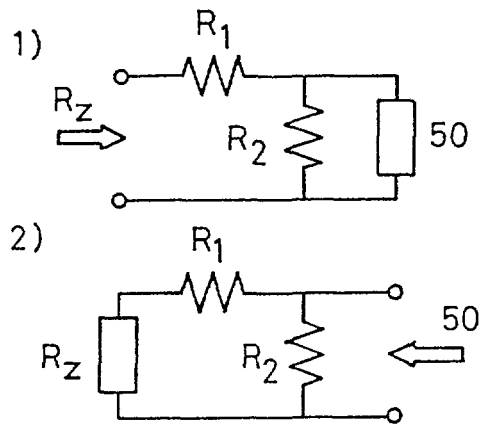

R_z ; characteristic impedance of T.W. Helix

With Fig. 1)

$$R_z = R_1 + \frac{50 \cdot R_2}{R_2 + 50}$$

and with Fig. 2)

$$50 = \frac{R_2 \cdot (R_1 + R_z)}{R_1 + R_2 + R_z} \quad ,$$

then,

$$R_1 = (R_z - 50) \, [\, R_z / (R_z - 50) \,]^{1/2}$$

and

$$R_2 = 50 \cdot [\, R_z / (R_z - 50) \,]^{1/2}$$

Fig. 3-8

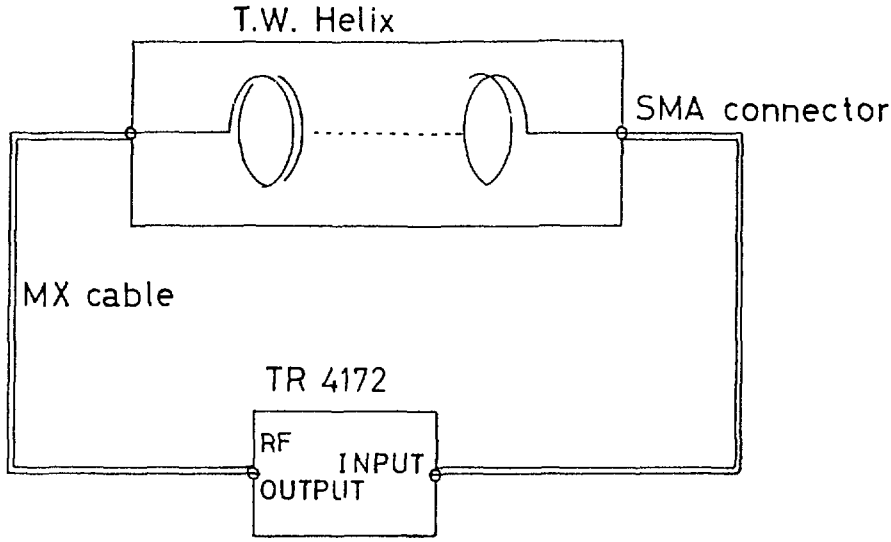

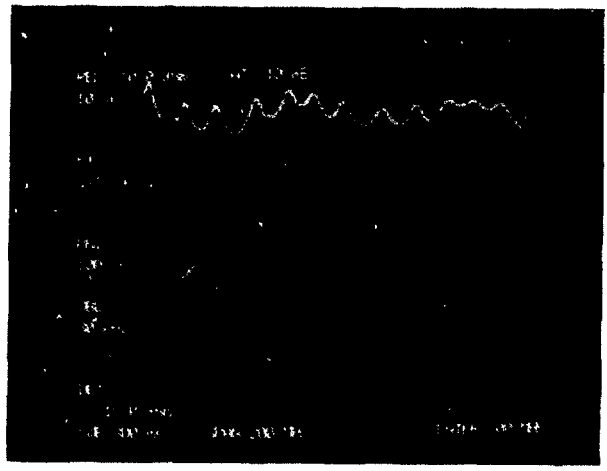

Fig. 3-9-a

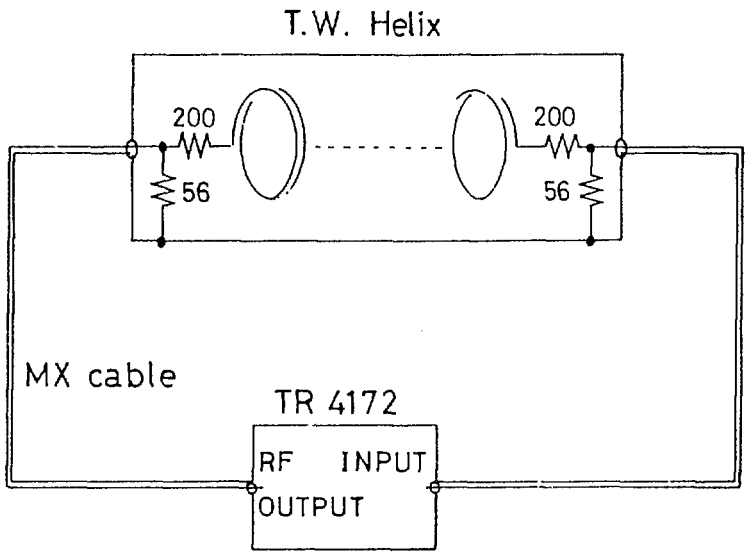

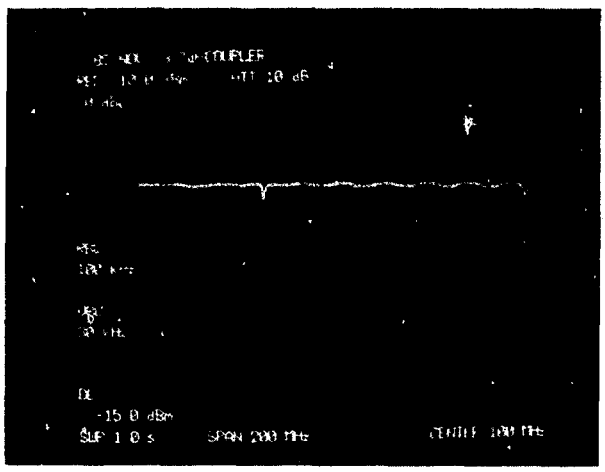

Fig. 3-9-b

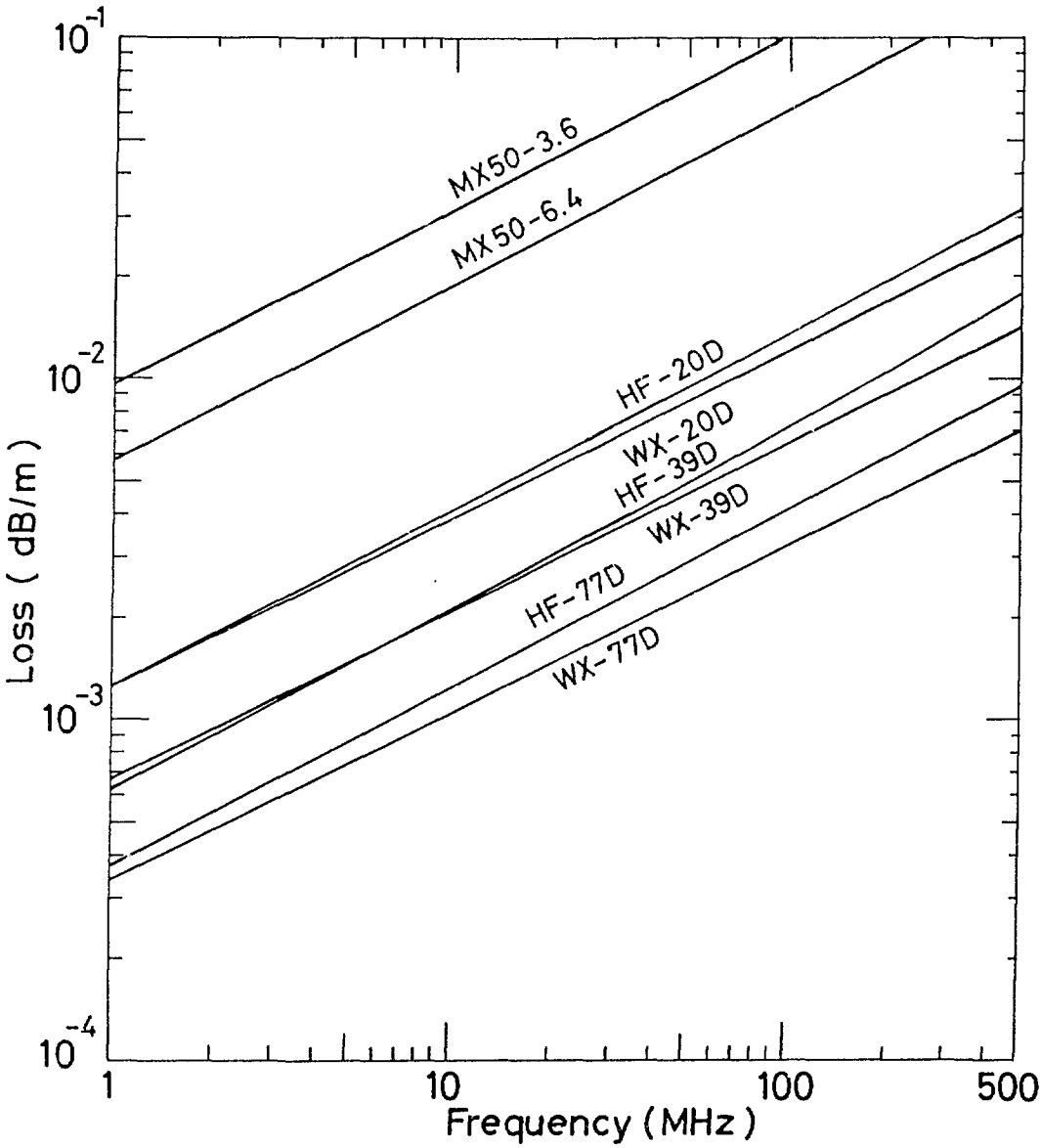
10^{-1}
10^{-2}
10^{-3}
10^{-4}
Loss (dB/m)
MX50-3.6
MX50-6.4
HF-20D
WX-20D
HF-39D
WX-39D
HF-77D
WX-77D
1
10
100
500
Frequency (MHz)

Fig. 4-1

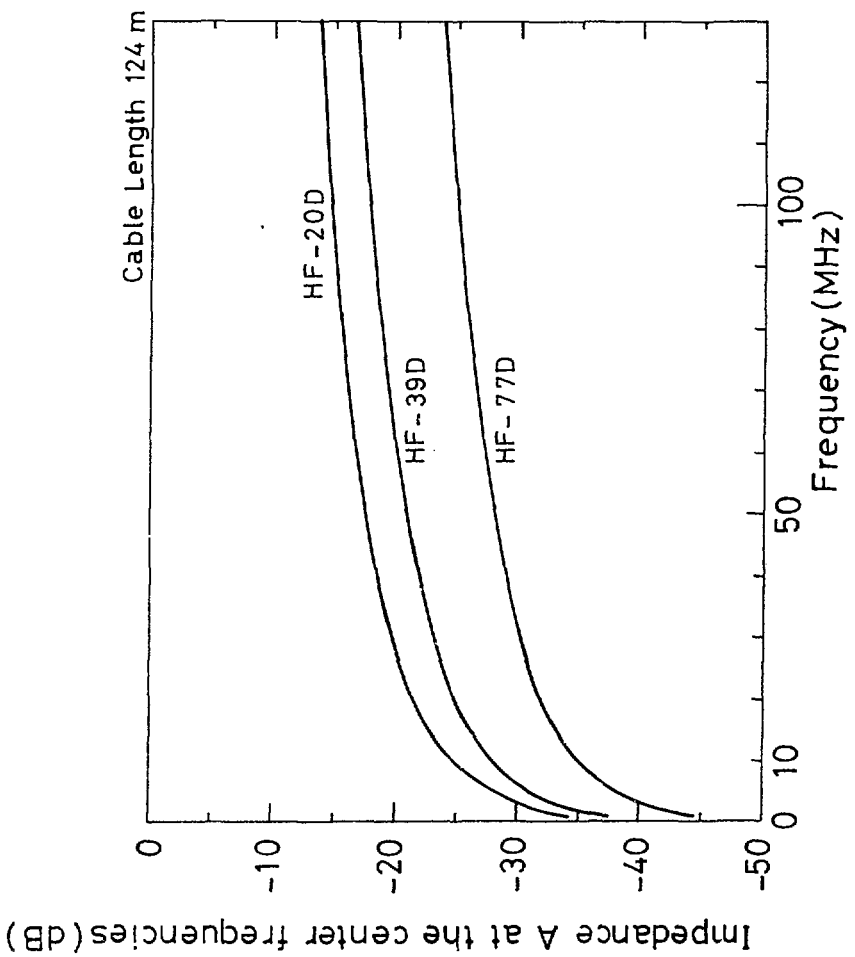
Cable Length 124 m
HF-20D
HF-39D
HF-77D
0
-10
-20
-30
-40
-50
0
10
50
100
Frequency (MHz)
Impedance A at the center frequencies (dB)

Fig. 4-2

Notch Filter (I)

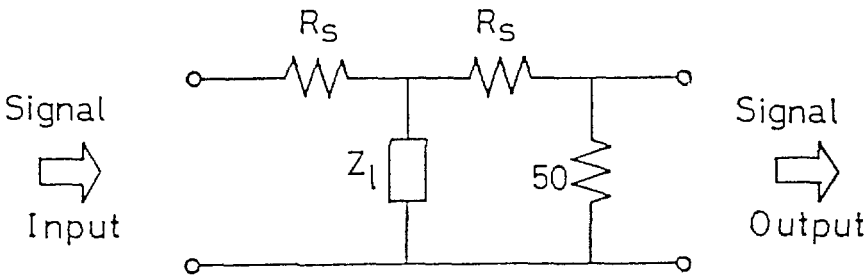

Impedance of Notch Filter Z_ℓ

$$Z_\ell = \begin{cases} Z_\ell^S = Z_0 \tanh (\gamma \ell) \ ; \text{ short end} \\ Z_\ell^O = Z_0 \coth (\gamma \ell) \ ; \text{ open end} \end{cases} .$$

Z_0 ; characteristic impedance of the cable

Fig. 4-3

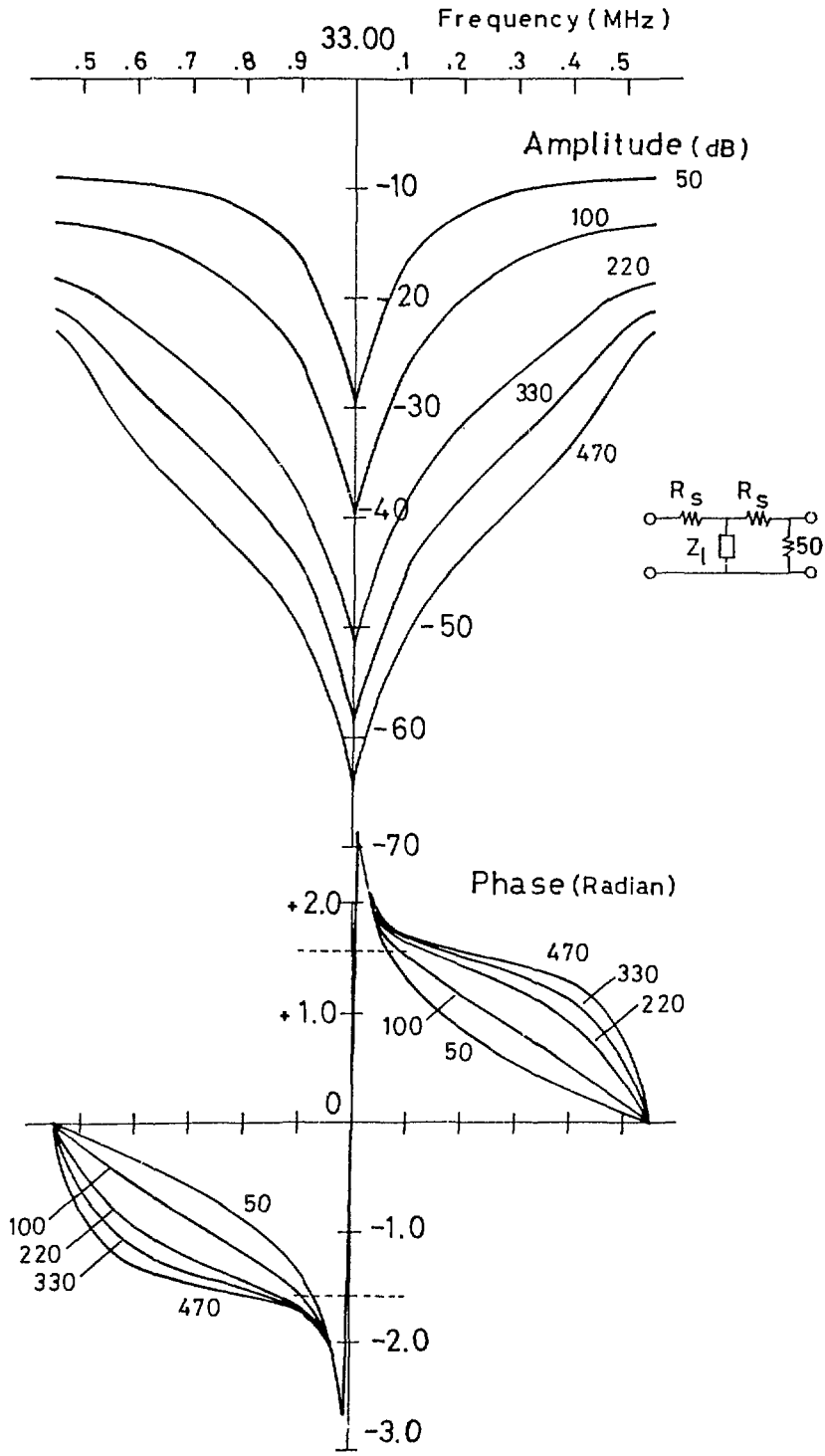
Frequency (MHz)
33.00
.5 .6 .7 .8 .9 .1 .2 .3 .4 .5
Amplitude (dB)
-10
-20
-30
-40
-50
-60
-70
50
100
220
330
470
Rs Rs
Zl
50
Phase (Radian)
+2.0
+1.0
0
-1.0
-2.0
-3.0
470
330
220
100
50
50
100
220
330
470

Fig. 4-4

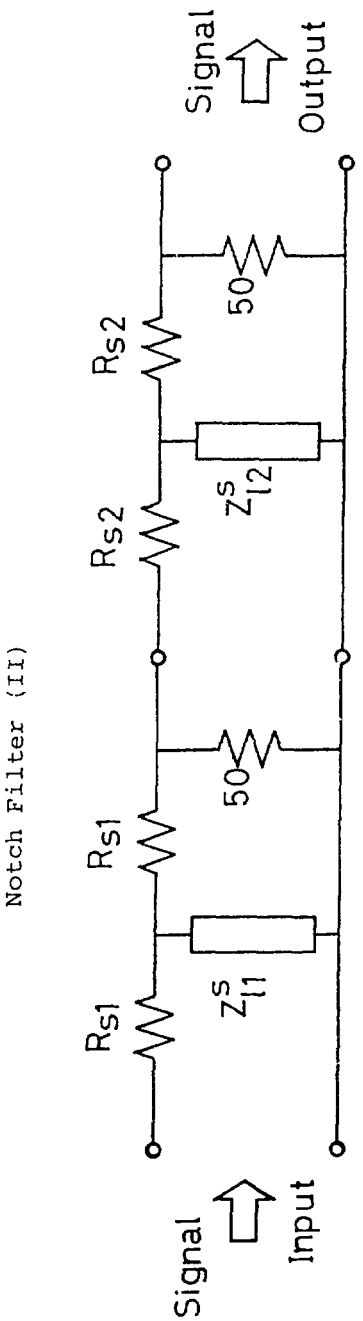
Notch Filter (II)
Signal
Input
Signal
Output
50
50
R_{s1}
R_{s1}
R_{s2}
R_{s2}
Z^s_{l1}
Z^s_{l2}

Fig. 4-5

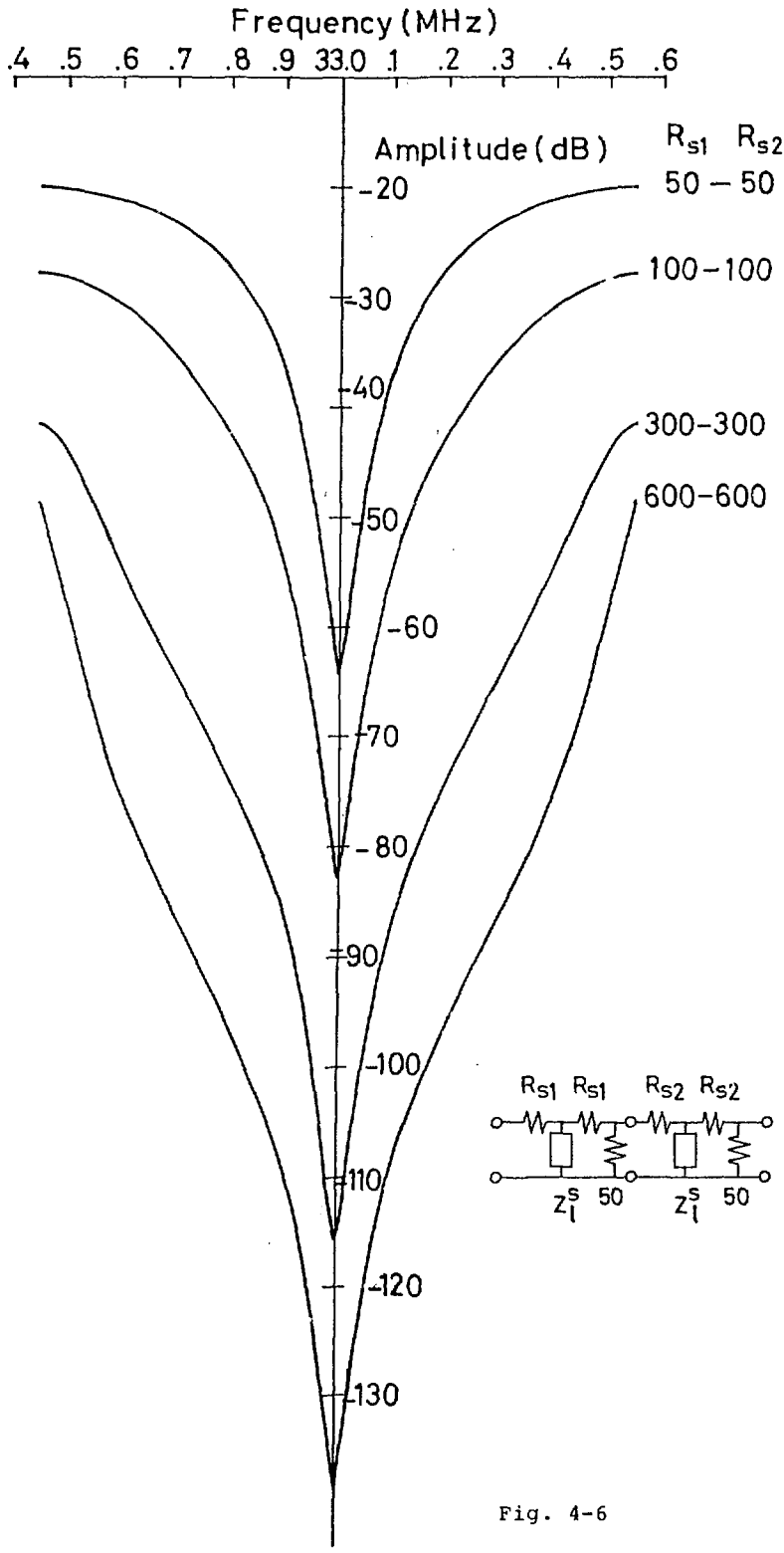
Frequency (MHz)
.4 .5 .6 .7 .8 .9 33.0 .1 .2 .3 .4 .5 .6
Amplitude (dB)
-20
-30
-40
-50
-60
-70
-80
-90
-100
-110
-120
-130
Rs1 Rs2
50 — 50
100-100
300-300
600-600
Rs1 Rs1 Rs2 Rs2
Z1s 50 Z1s 50

Fig. 4-6

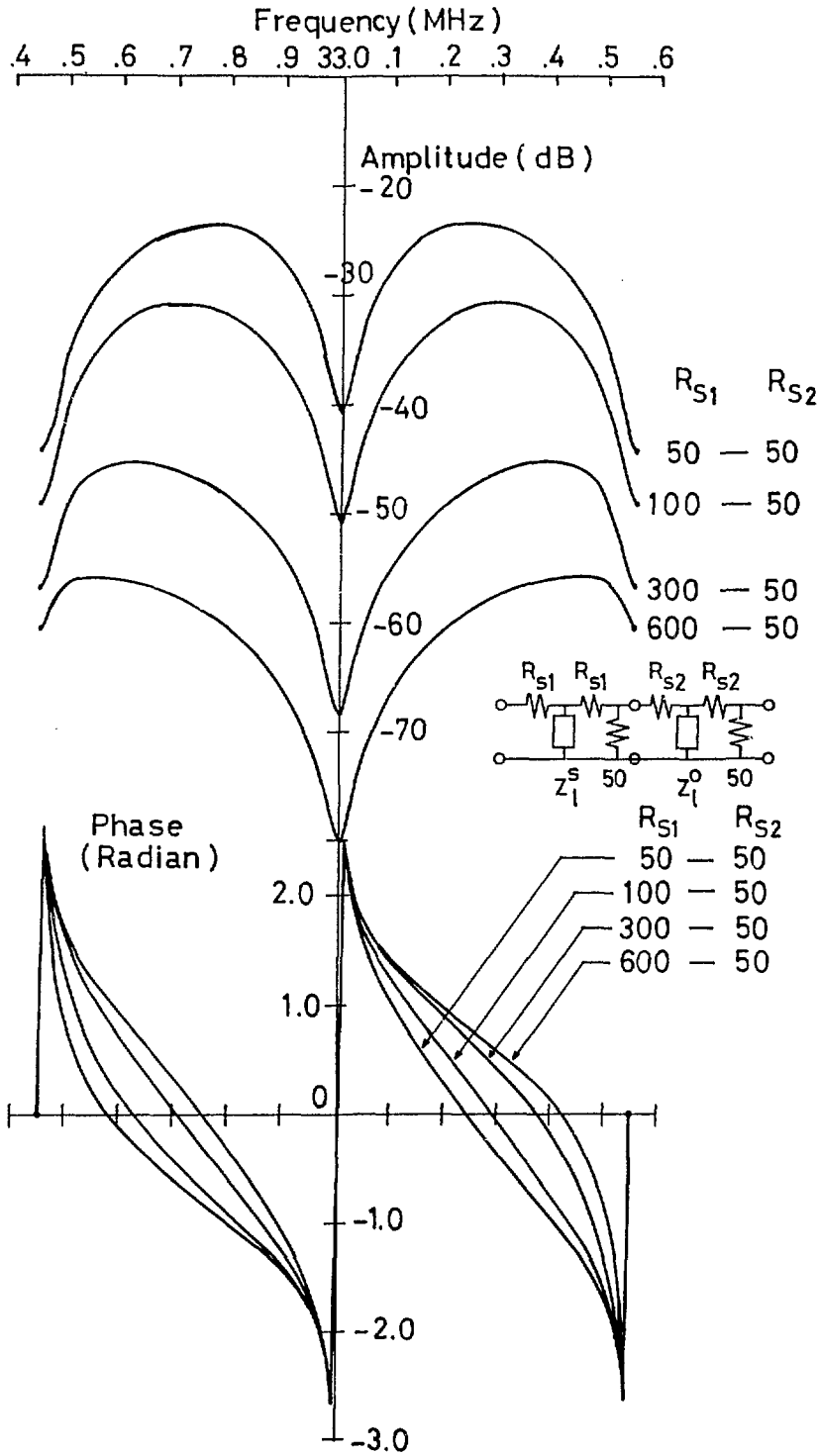
Frequency (MHz)
.4 .5 .6 .7 .8 .9 33.0 .1 .2 .3 .4 .5 .6
Amplitude (dB)
-20
-30
-40
-50
-60
-70
R_{S1} R_{S2}
50 — 50
100 — 50
300 — 50
600 — 50
R_{S1} R_{S1} R_{S2} R_{S2}
Z_l^s 50 Z_l^o 50
Phase
(Radian)
2.0
1.0
0
-1.0
-2.0
-3.0
R_{S1} R_{S2}
50 — 50
100 — 50
300 — 50
600 — 50

Fig. 4-7

Short End Notch Filter (I)

R_s = 100 Ω

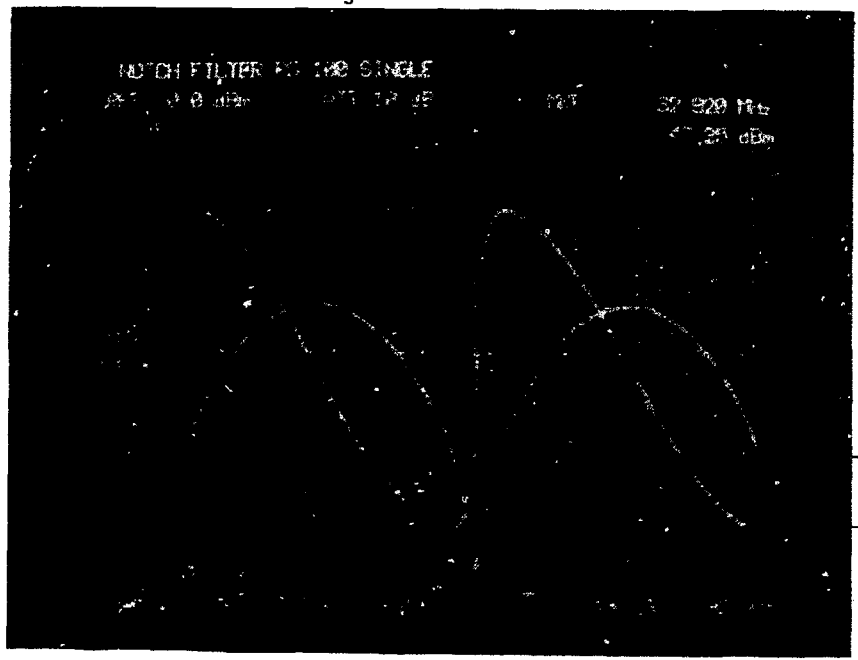

Amplitude ; 5 dB/div.

Phase ; 20 °/div.

Fig. 4-8

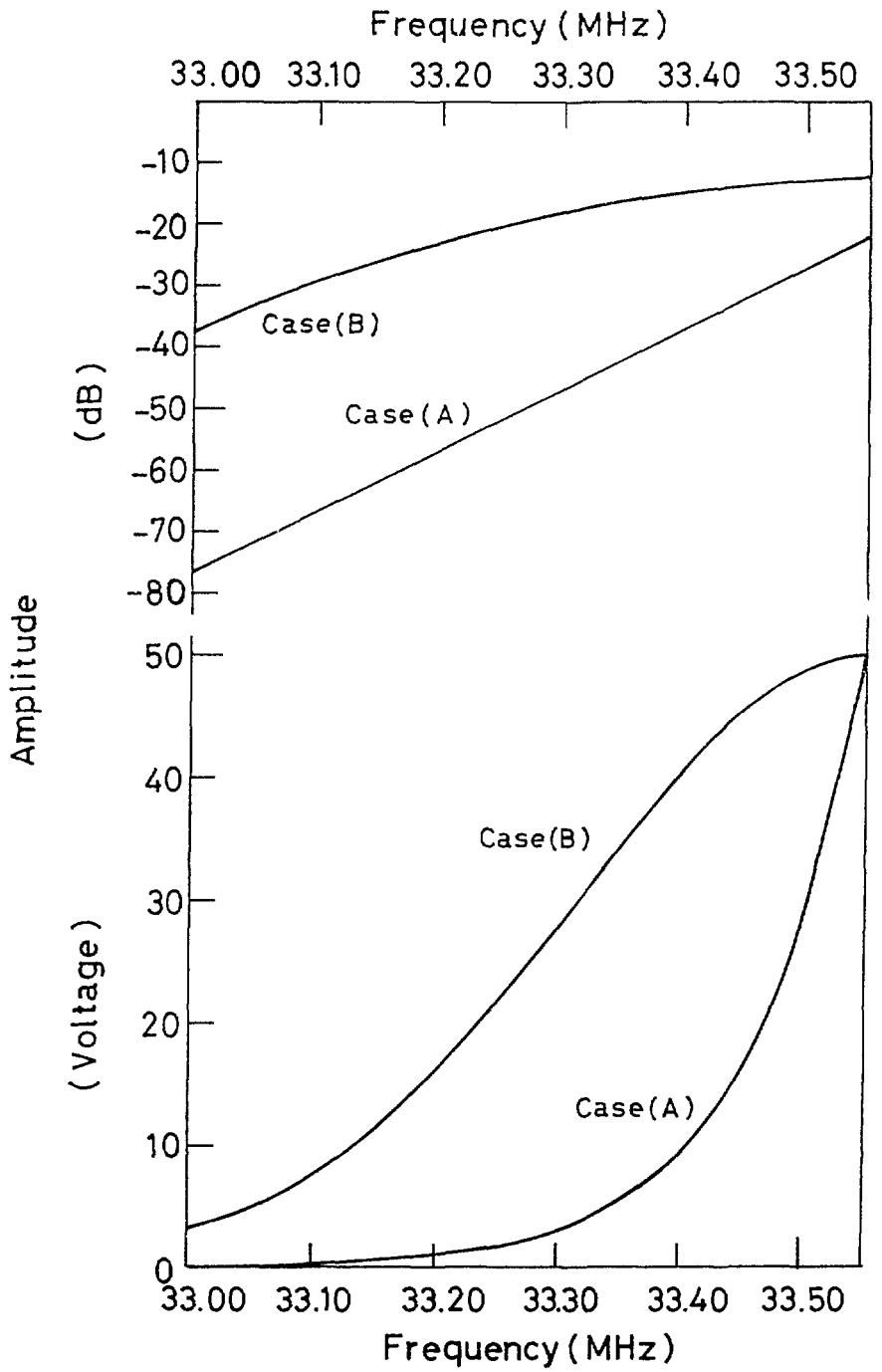
Frequency (MHz)
33.00
33.10
33.20
33.30
33.40
33.50
-10
-20
-30
-40
-50
-60
-70
-80
(dB)
Case(B)
Case(A)
Amplitude
50
40
30
20
10
0
(Voltage)
Case(B)
Case(A)
33.00
33.10
33.20
33.30
33.40
33.50
Frequency (MHz)

Fig. 5-1

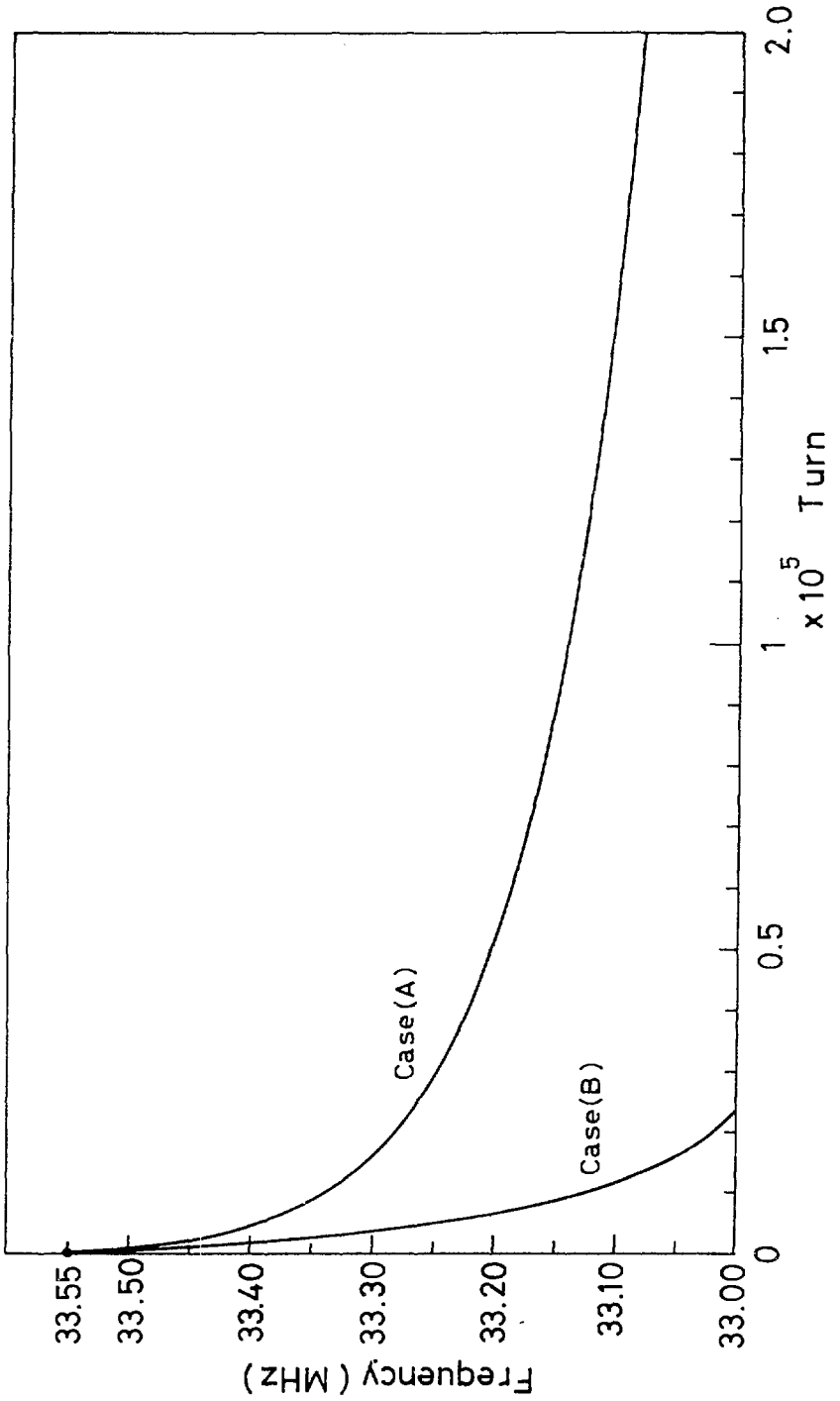
Frequency (MHz)
33.55
33.50
33.40
33.30
33.20
33.10
33.00
0
0.5
1
1.5
2.0
x 10^5 Turn
Case(A)
Case(B)

Fig. 5-2

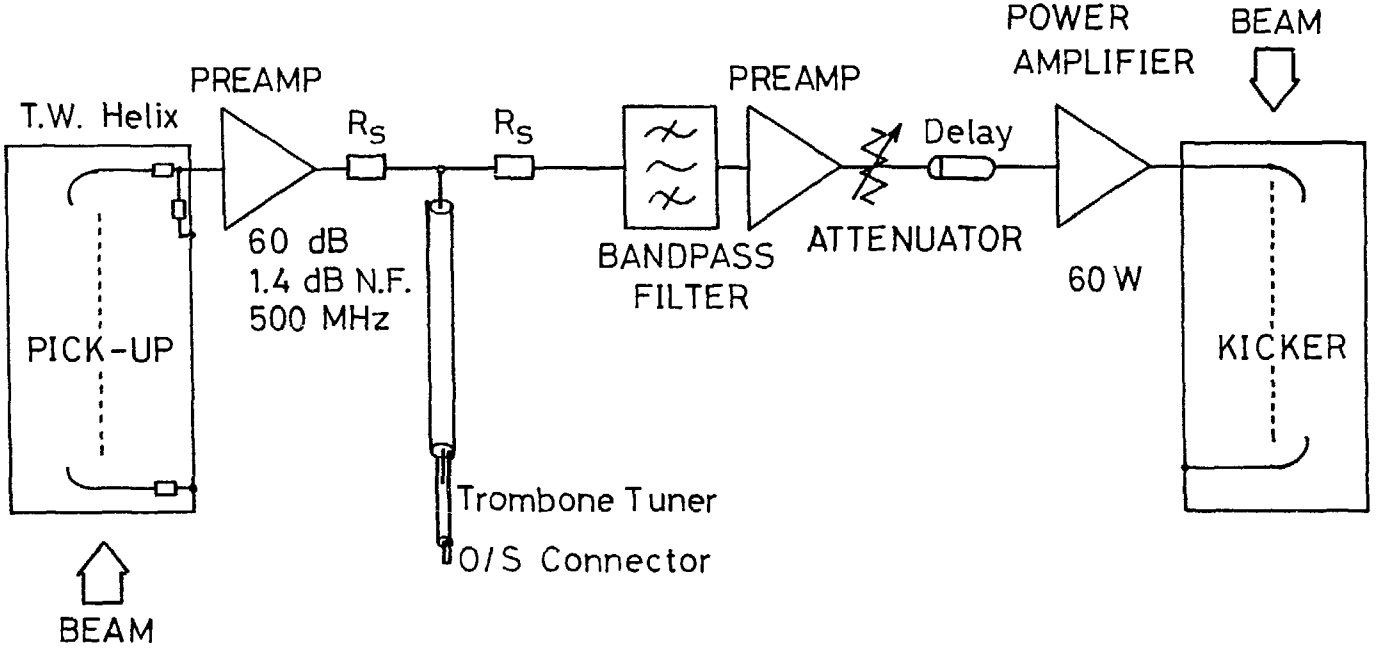
POWER
AMPLIFIER
BEAM
PREAMP
PREAMP
T.W. Helix
R_S
R_S
Delay
60 dB
1.4 dB N.F.
500 MHz
BANDPASS
FILTER
ATTENUATOR
60 W
PICK-UP
KICKER
Trombone Tuner
O/S Connector
BEAM

Fig. 6-1

Coaxial Switch

PN 82152-919C70100 (SN. E1418)

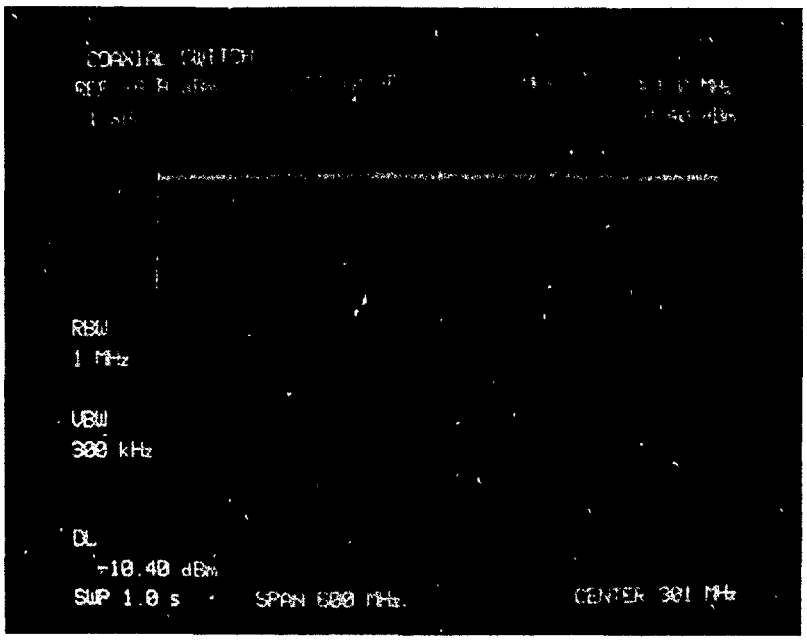

Loss ; 1 dB/div.

DL Level ;
Through Level

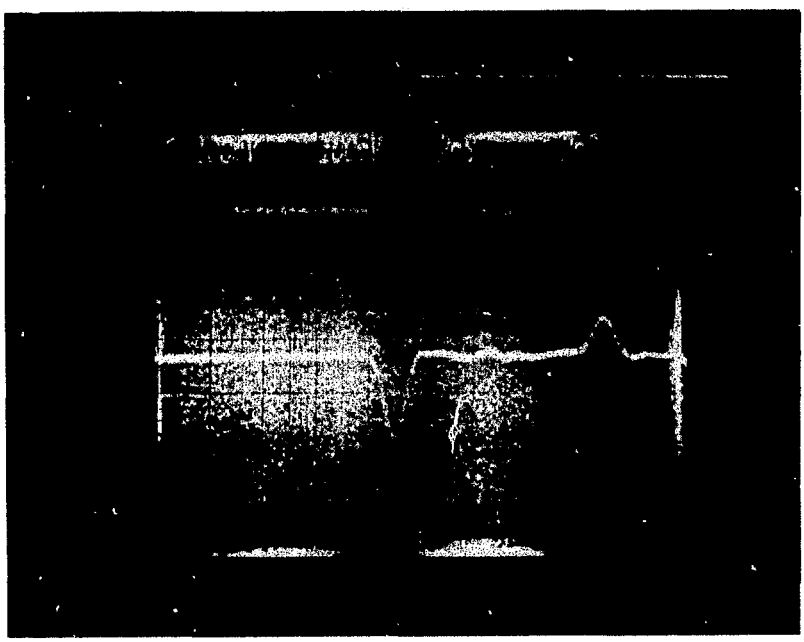

Delay Time ;
2nsec/div.

Delay Time of this Switch < 0.1 nsec .

Fig. 6-2

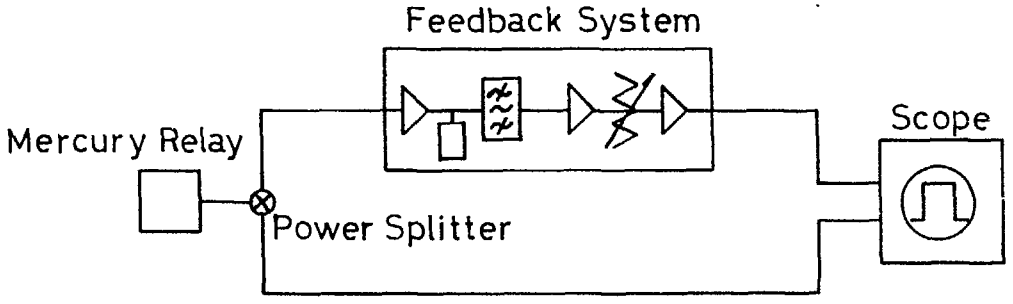

Fig. 6-3

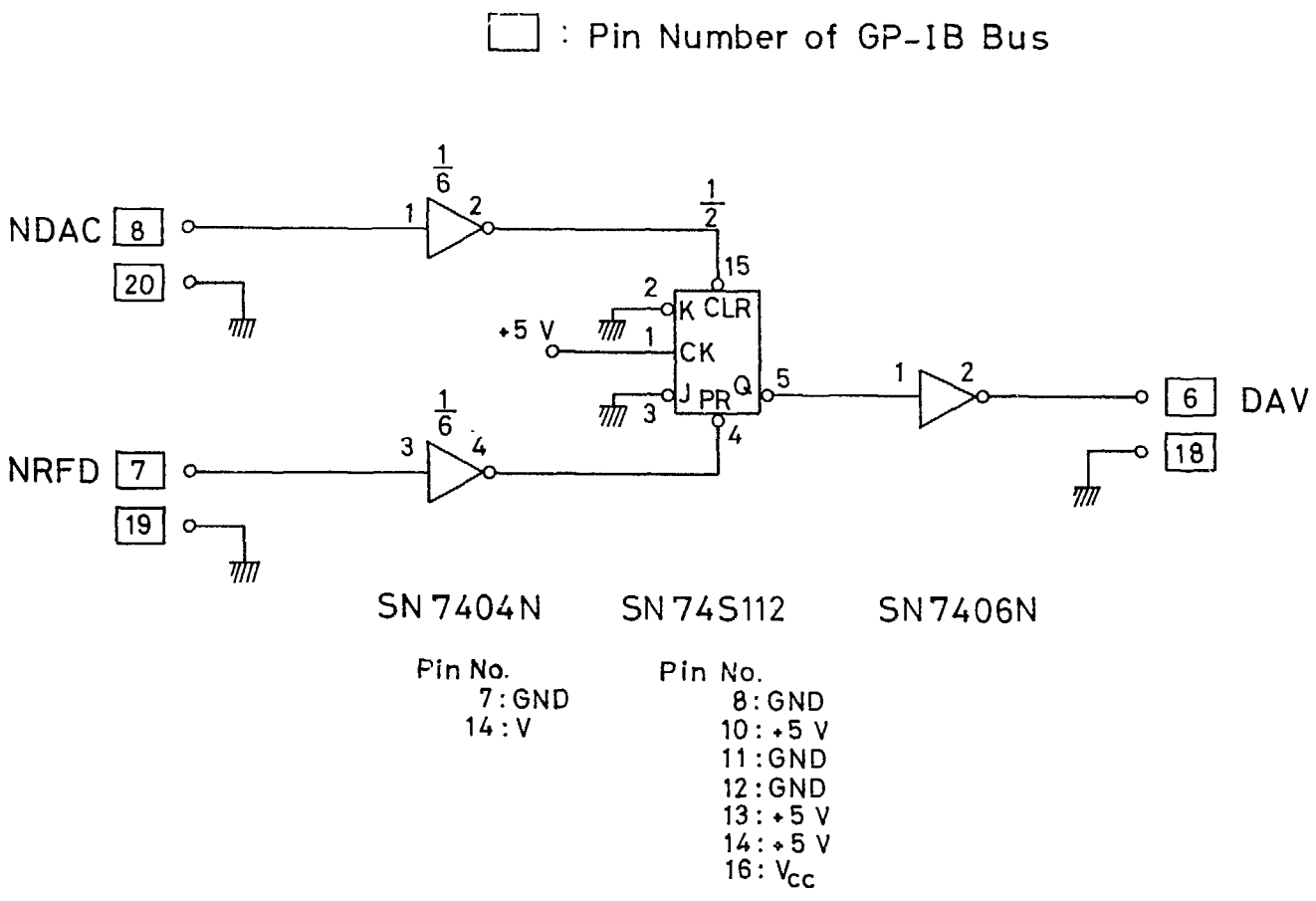
: Pin Number of GP-IB Bus
NDAC
8
20
NRFD
7
19
1/6
1/6
1/2
+5 V
K CLR
CK
J PR
Q
6
DAV
18
SN7404N
SN74S112
SN7406N
Pin No.
7 : GND
14 : V
Pin No.
8 : GND
10 : +5 V
11 : GND
12 : GND
13 : +5 V
14 : +5 V
16 : Vcc

Fig. 7-1

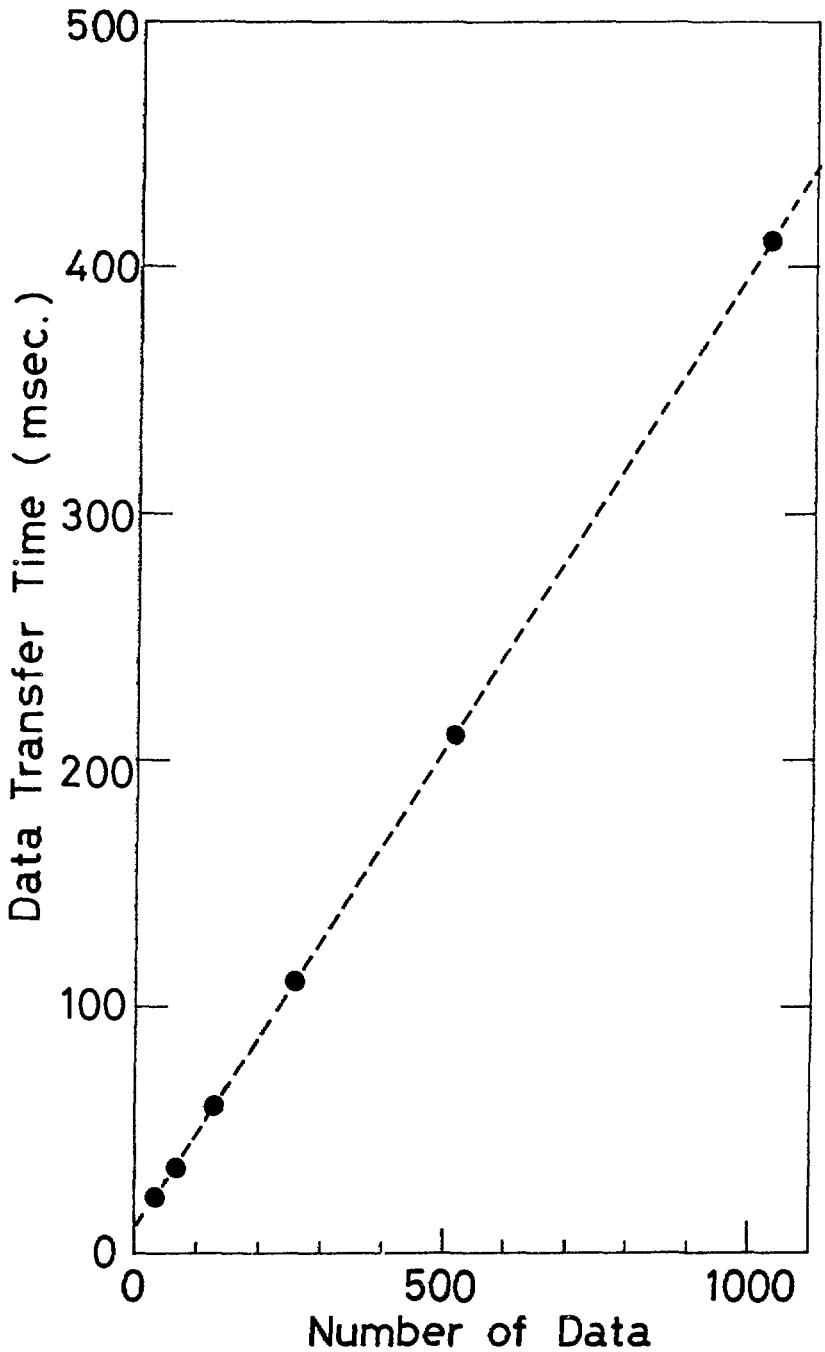
500
400
300
200
100
0
Data Transfer Time (msec.)
0
500
1000
Number of Data

Fig. 7-2

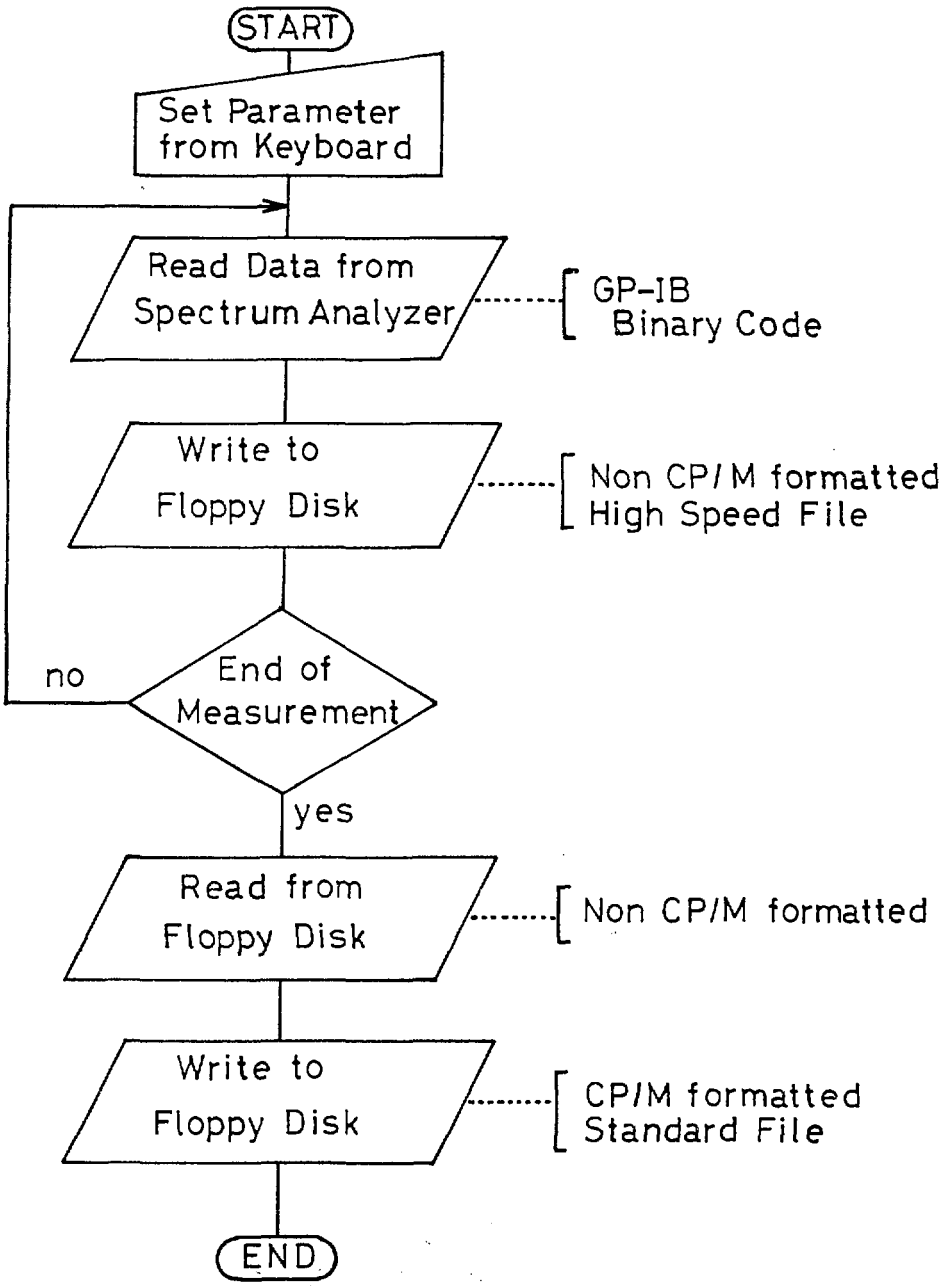
START
Set Parameter from Keyboard
Read Data from Spectrum Analyzer
GP-IB Binary Code
Write to Floppy Disk
Non CP/M formatted High Speed File
no
End of Measurement
yes
Read from Floppy Disk
Non CP/M formatted
Write to Floppy Disk
CP/M formatted Standard File
END

Fig. 7-3

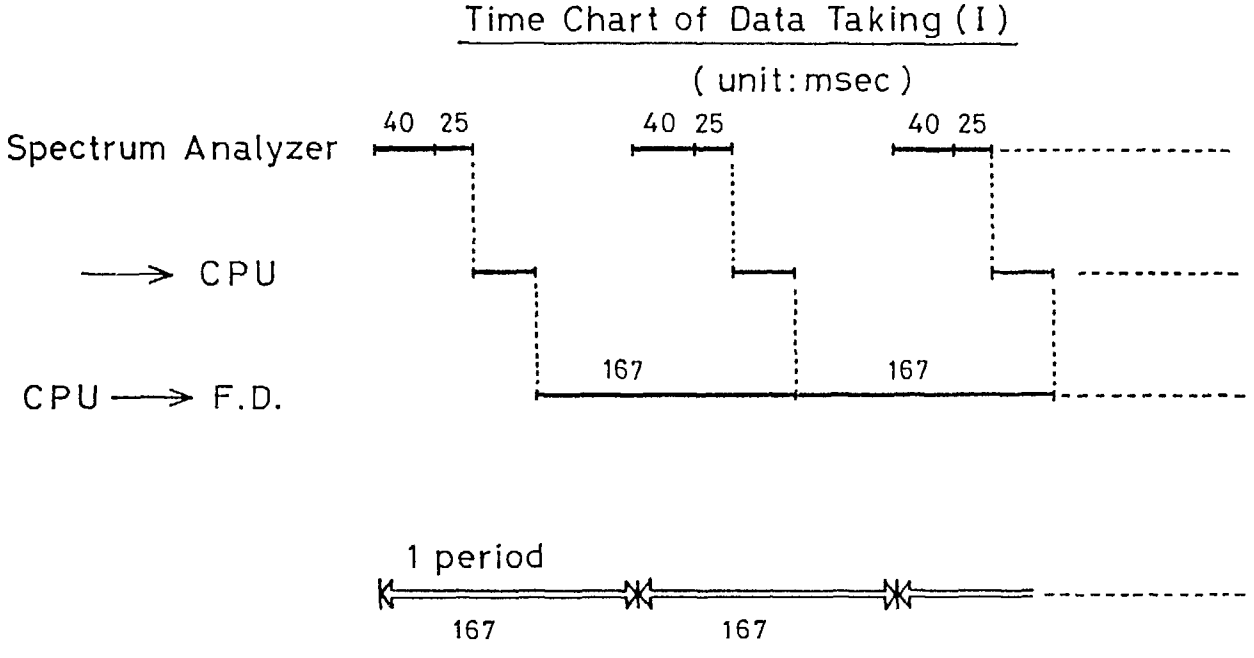
Time Chart of Data Taking (I)
(unit: msec)
Spectrum Analyzer
40 25
40 25
40 25
CPU
CPU → F.D.
167
167
1 period
167
167

Fig. 7-4

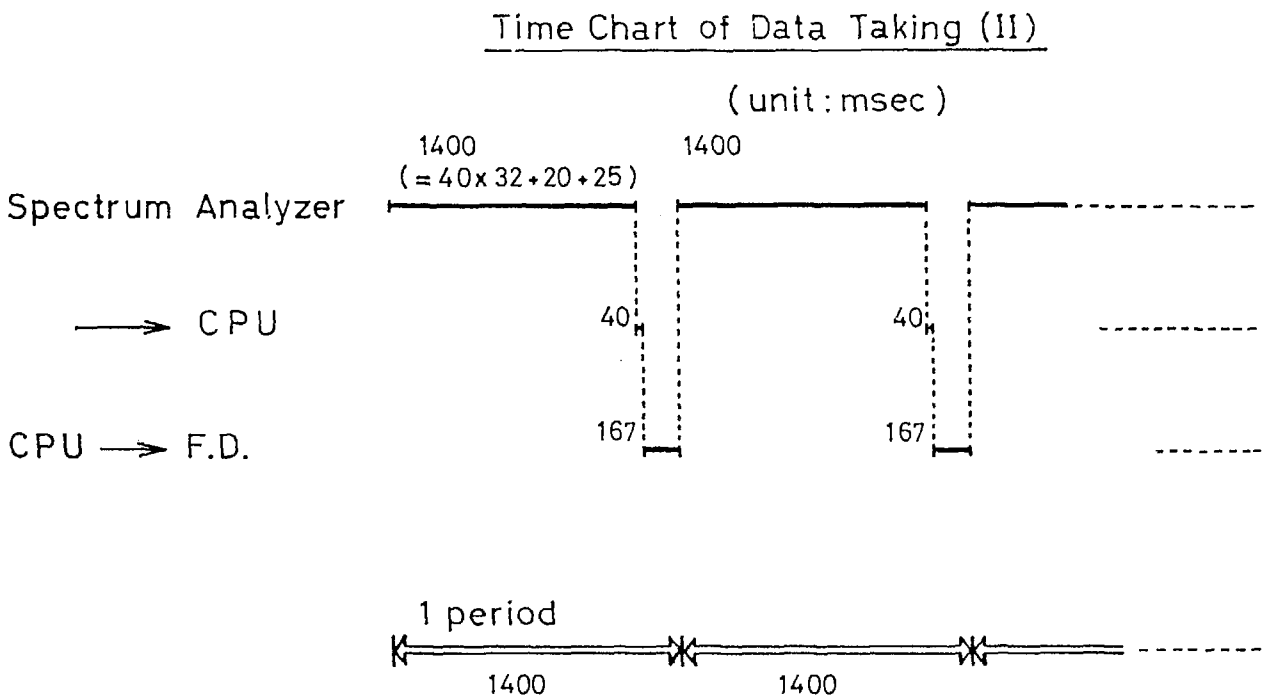
Time Chart of Data Taking (II)
(unit : msec)
1400
(= 40 x 32 + 20 + 25)
1400
Spectrum Analyzer
CPU
40
40
CPU → F.D.
167
167
1 period
1400
1400

Fig. 7-5

Parameter List of TARN for Proton Beam

General		
Beam energy (for proton)		7.00 MeV
Magnetic field		B = 2.871 kG
Bending radius		ρ = 1.333 m
Mean orbit radius		R = 5.06 m
Revolution frequency		f_0= 1.145 MHz
Betatron ν values		ν_x = 2.250
		ν_y = 2.200
vacuum pressure		1 x 10^{-10} torr
Injection scheme		Multiturn injection
Magnet and Lattice		
Number of normal cells		8
Number of superperiods		8
Number of long straight sections		8
Periodic structure		Q_F B Q_D O
Bending magnets		
Number		8
Gap		70 mm
Pole width		258 mm
Good field aperture		40 x 170 mm^2
Quadrupole magnets		
Number		16
Length		0.20 m
Field gradient		k_F = 0.065 kG/cm
		k_D = 0.110 kG/cm
Momentum compaction factor		Maximum = 1.70 m
		Minimum = 1.01 m
		Average = 1.41 m
Betatron amplitude function	(x)	(y)
	Maximum = 4.94 m	5.51 m
	Minimum = 1.08 m	1.18 m
RF Stacking System		
Frequency		8.0 MHz
Harmonic number		7
Maximum accelerating voltage		1.1 kV
Number of cavities		1
Total RF power		1.3 kW
Stacking parameter		
Momentum spread of the stacked beam		~ 3 %
Momentum difference between the injection orbit and stack top		~ 5 %
Repetition rate		30 Hz
RF stacking number (ordinary)		20

Table 1

Parameter List of T.W. Helix in the case of ℓ = 6 cm

Nagaoka Factor n	Z_0 (Ω)	b (cm)	Monitor Length z_d (m)
0.959	240	9.7	1.2
0.920	230	9.5	0.6
0.900	225	9.4	0.5
0.884	221	9.3	0.4

Table 3-1

Table 4-1

Specifications of some HF-Cables

Cable No.	Shortening Ratio of Wave Length (%)	Loss at 20°C (max.) (dB/100m) 30 MHz	100 MHz	300 MHz	Weight (kg/m)	Cable Length Fundamental Frequency 1.10 MHz	1.14 MHz
HF-20D	91	0.72	1.34	2.40	0.9	124.01	119.66
HF-39D	91	0.38	0.72	1.34	1.9	"	"
HF-77D	94.5	0.22	0.41	0.74	3.6	128.78	124.26

DRUM ; 170 kg (1750 mmϕ x 940 mm width)

See ; Hitachi Cable, Ltd.
RADIO FREQUENCY TRANSMISSION CABLES CAT. NO. F_4-611$_E$

	Delay Time
MX 6.4 Coaxial Cable	4.78 nsec/m
Attenuator (3200-2)	
" (1462)	1.8 nsec
" (1542)	1.8 nsec
Pre-Amplifier (TRONTECH)	
W 500C (M22901)	1.6 nsec
" (M22903)	1.6 nsec
W 500EF (M22901)	2.3 nsec
" (M22902)	2.3 nsec
" (M21701)	2.9 nsec
" (M21702)	2.7 nsec
W 1G2H (M22901)	1.0 nsec
" (M22902)	1.0 nsec
Pass-Filter	
XHDP10-4GG (H. P. F.)	1.0 nsec
LHP200-4GG (L. P. F.)	7.0 nsec

Table 6-1

Frequency

Measuring Range	; 50 Hz to 1800 MHz (DC couple)
	; 10 kHz to 1800 MHz (AC couple)
Center Frequency Accuracy	; ± (1 % of freq. span ± 20 Hz)
Oscillator Stability	
Aging Rate	; 5×10^{-10} /day
Temp. Stability (25°C±25°C)	; ± 5×10^{-9} /day
Resolution Bandwidth	; 10 Hz to 1 MHz in 1 and 3 steps.
Bandwidth Accuracy	; ± 20 % (at 3 dB bandwidth)
Frequency Stability	; Less than 30 Hz_{p-p} /min. (frequency span 50 kHz)

Amplitude

Measuring Range	; -130 dB_m to +20 dB_m
Reference Level Accuracy	; ± 1$dB_{max.}$
Dynamic Range	
Center Freq. 20 MHz	
Input -30 dB_m	; -80 dB
-40 dB_m	; -90 dB
Center Freq. 20 MHz	
Input -30 dB_m	; -60 dB
Noise Level	; -130 dB_m

resolution bandwidth 10 Hz, video filter 1 Hz, center frequency 1 MHz

Sweep

Sweep Time	; 50 msec 1000 sec

Input

Maximum Input Level	; +20 dB_m
	; 0 V $DC_{max.}$ (DC couple)
	; ±25 V $DC_{max.}$ (AC couple)

Output

GP-IB Data Output and Remote Control

Table 7-1

Specification of THE BOX

Size	;	276 (W) x 206 (H) x 414 (D)
Weight	;	13.5 kg
CPU	;	Z80A (4 MHz)
Boot ROM	;	i2764 (8 Kbite)
RAM	;	64 K
Serial Interface	;	4 ch. RS232c standard
		TTL 20mA current loop (1 ch.)
		Boo Rate 75 19200 BPS
Printer Interface	;	Centronics Interface 1 ch.
Floppy Disk Interface	;	8" FDD x2 standard

Table 7-2